8   Gutzwiller Density Functional Theory

Florian Gebhard
Department of Physics
Philipps Universität Marburg, Germany

Contents

1 Introduction

Density Functional Theory (DFT) is the workhorse of electronic structure theory. Based on the Hohenberg-Kohn and Kohn-Sham theorems [1], the ground-state properties of an interacting many-electron system are calculated from those of an effective single-particle problem that can be solved numerically. An essential ingredient in DFT is the so-called exchange-correlation potential which, however, is unknown and sensible approximations must be devised, e.g., the local (spin) density approximation, L(S)DA. In this way, the electronic properties of metals were calculated systematically [2]. Unfortunately, the L(S)DA leads to unsatisfactory results for transition metals and their compounds. The electrons in the narrow $3d$, or $4f/5f$, bands experience correlations that are not covered by current exchange-correlation potentials.

For a more accurate description of electronic correlations in narrow bands, Hubbard-type models [3,4] have been put forward. However, simplistic model Hamiltonians can describe limited aspects of real materials at best, while, at the same time, they reintroduce the full complexity of the many-body problem. Recently, new methods were developed that permit the (numerical) analysis of multi-band Hubbard models and, moreover, can be combined with DFT, specifically, the LDA+U method [5], the LDA+DMFT (Dynamical Mean-Field Theory) [6,7], and the Gutzwiller variational approach [8–11]. The LDA+U approach treats atomic interactions on a mean-field level so that it is computationally cheap but it ignores true many-body correlations. The DMFT becomes formally exact for infinite lattice coordination number, $Z \to \infty$, but it requires the self-consistent solution of a dynamical impurity problem that is numerically very demanding. The Gutzwiller DFT is based on a variational treatment of local many-body correlations. Expectation values can be calculated for $Z \to \infty$ without further approximations, and the remaining computational problem remains tractable.

In this chapter, we present a formal derivation of the Gutzwiller DFT as a generic extension of the DFT. Our formulae apply for general Gutzwiller-correlated wave functions and reproduce expressions used previously [9,10] as special cases. We provide results for nickel in the face-centered cubic (fcc) structure and for iron in its body-centered cubic (bcc) ground state. The Gutzwiller DFT results for the lattice constant, the magnetic spin-only moment, and the bulk modulus agree very well with experiments. Moreover, the quasi-particle bandstructure from Gutzwiller DFT is in satisfactory agreement with data from Angle-Resolved Photo-Emission Spectroscopy (ARPES). As found earlier [8–10], the Gutzwiller DFT overcomes the limitations of DFT for the description of transition metals.

In Sect. 2 we recall the derivation of Density Functional Theory (DFT) as a variational approach to the many-body problem and its mapping to an effective single-particle reference system (Kohn-Sham scheme). In Sect. 3 we extend our derivation to many-particle reference systems. We formulate the Gutzwiller density functional whose minimization leads to the Gutzwiller–Kohn-Sham Hamiltonian. The theory is worked out in the limit of large coordination number, $Z \to \infty$, where explicit expressions for the Gutzwiller density functional are available. In Sect. 4 we present results for fcc nickel ($Z = 12$) and for bcc iron ($Z = 8$). Summary and conclusions, Sect. 5, close our presentation. Some technical details are deferred to the appendix. This work is based on Refs. [12,13]. Further on, excerpts are taken without explicit citations.

2 Density Functional Theory

We start our presentation with a concise derivation of Density Functional Theory that can readily be extended to the Gutzwiller Density Functional Theory.

2.1 Many-particle Hamiltonian and Ritz variational principle

The non-relativistic many-particle Hamiltonian for electrons with spin $\sigma = \uparrow, \downarrow$ reads ($\hbar \equiv 1$)

$$
\begin{aligned}
\hat{H} &= \hat{H}_{\text{band}} + \hat{H}_{\text{int}} \,, \\
\hat{H}_{\text{band}} &= \sum_{\sigma} \int \mathrm{d}\mathbf{r}\, \hat{\Psi}_{\sigma}^{\dagger}(\mathbf{r}) \left(-\frac{\Delta_{\mathbf{r}}}{2m} + U(\mathbf{r}) \right) \hat{\Psi}_{\sigma}(\mathbf{r}) \,, \\
\hat{H}_{\text{int}} &= \sum_{\sigma,\sigma'} \int \mathrm{d}\mathbf{r} \int \mathrm{d}\mathbf{r}'\, \hat{\Psi}_{\sigma}^{\dagger}(\mathbf{r})\hat{\Psi}_{\sigma'}^{\dagger}(\mathbf{r}')\, V(\mathbf{r} - \mathbf{r}')\, \hat{\Psi}_{\sigma'}(\mathbf{r}')\hat{\Psi}_{\sigma}(\mathbf{r})
\end{aligned} \tag{1}
$$

with

$$
V(\mathbf{r} - \mathbf{r}') = \frac{1}{2} \frac{e^2}{|\mathbf{r} - \mathbf{r}'|} \,. \tag{2}
$$

The electrons experience the periodic potential of the ions, $U(\mathbf{r})$, and their mutual Coulomb interaction, $V(\mathbf{r} - \mathbf{r}')$. The total number of electrons is $N = N_{\uparrow} + N_{\downarrow}$. According to the Ritz variational principle, the ground state of a Hamiltonian $\hat{H}$ can be obtained from the minimization of the energy functional

$$
E\left[\{|\Psi\rangle\}\right] = \langle \Psi | \hat{H} | \Psi \rangle \tag{3}
$$

in the subset of normalized states $|\Psi\rangle$ in the Hilbert space with N electrons, $\langle \Psi | \Psi \rangle = 1$.

2.2 Levy's constrained search

The minimization of the energy functional (3) is done in two steps, the constrained search [14], Sect. 2.2.1, and the minimization of the density functional, Sect. 2.2.2. To this end, we consider the subset of normalized states $|\Psi^{(n)}\rangle$ with fixed electron densities $n_{\sigma}(\mathbf{r})$,

$$
n_{\sigma}(\mathbf{r}) = \langle \Psi^{(n)} | \hat{\Psi}_{\sigma}^{\dagger}(\mathbf{r})\hat{\Psi}_{\sigma}(\mathbf{r}) | \Psi^{(n)} \rangle \,. \tag{4}
$$

In the following we accept 'physical' densities only, i.e., those $n_{\sigma}(\mathbf{r})$ for which states $|\Psi^{(n)}\rangle$ can actually be found. For the subset of states $|\Psi^{(n)}\rangle$ we define the electronic Hamiltonian

$$
\hat{H}_{\text{e}} = \hat{H}_{\text{kin}} + \hat{V}_{\text{xc}} \,, \tag{5}
$$

$$
\hat{H}_{\text{kin}} = \sum_{\sigma} \int \mathrm{d}\mathbf{r}\, \hat{\Psi}_{\sigma}^{\dagger}(\mathbf{r}) \left(-\frac{\Delta_{\mathbf{r}}}{2m} \right) \hat{\Psi}_{\sigma}(\mathbf{r}) \,, \tag{6}
$$

$$
\begin{aligned}
\hat{V}_{\text{xc}} = \sum_{\sigma,\sigma'} \int \mathrm{d}\mathbf{r} \int \mathrm{d}\mathbf{r}'\, V(\mathbf{r} - \mathbf{r}') &\Big[\hat{\Psi}_{\sigma}^{\dagger}(\mathbf{r})\hat{\Psi}_{\sigma'}^{\dagger}(\mathbf{r}')\hat{\Psi}_{\sigma'}(\mathbf{r}')\hat{\Psi}_{\sigma}(\mathbf{r}) \\
&- \hat{\Psi}_{\sigma}^{\dagger}(\mathbf{r})\hat{\Psi}_{\sigma}(\mathbf{r})n_{\sigma'}(\mathbf{r}') - \hat{\Psi}_{\sigma'}^{\dagger}(\mathbf{r}')\hat{\Psi}_{\sigma'}(\mathbf{r}')n_{\sigma}(\mathbf{r}) + n_{\sigma}(\mathbf{r})n_{\sigma'}(\mathbf{r}') \Big] \,.
\end{aligned} \tag{7}
$$

Here, we extracted the Hartree terms from the Coulomb interaction H_{int} in eq. (1) so that $\hat{V}_{\text{xc}}$ contains only the so-called exchange and correlation contributions. In the subset of normalized states $|\Psi^{(n)}\rangle$ we define the functional

$$F\left[\{n_\sigma(\mathbf{r})\}, \{|\Psi^{(n)}\rangle\}\right] = \langle\Psi^{(n)}|\hat{H}_{\text{e}}|\Psi^{(n)}\rangle \; . \tag{8}$$

For fixed densities $n_\sigma(\mathbf{r})$, the Hamiltonian $\hat{H}_{\text{e}}$ defines an electronic problem where the periodic potential of the ions and the Hartree interaction are formally absent.

2.2.1 Constrained search

The formal task is to find the minimum of the energy functional F in (8) with respect to $|\Psi^{(n)}\rangle$,

$$\bar{F}\left[\{n_\sigma(\mathbf{r})\}\right] = \text{Min}_{\{|\Psi^{(n)}\rangle\}} F\left[\{n_\sigma(\mathbf{r})\}, \{|\Psi^{(n)}\rangle\}\right] \; . \tag{9}$$

Recall that the electron densities $n_\sigma(\mathbf{r})$ are fixed in this step. We denote the resulting optimal many-particle state by $|\Psi_0^{(n)}\rangle$. Thus, we may write

$$\bar{F}\left[\{n_\sigma(\mathbf{r})\}\right] = F\left[\{n_\sigma(\mathbf{r})\}, \{|\Psi_0^{(n)}\rangle\}\right] = \langle\Psi_0^{(n)}|\hat{H}_{\text{e}}|\Psi_0^{(n)}\rangle \; . \tag{10}$$

For later use, we define the corresponding functionals for the kinetic energy

$$K\left[\{n_\sigma(\mathbf{r})\}\right] = \langle\Psi_0^{(n)}|\hat{H}_{\text{kin}}|\Psi_0^{(n)}\rangle \tag{11}$$

and the exchange-correlation energy

$$E_{\text{xc}}\left[\{n_\sigma(\mathbf{r})\}\right] = \langle\Psi_0^{(n)}|\hat{V}_{\text{xc}}|\Psi_0^{(n)}\rangle \tag{12}$$

so that

$$\bar{F}\left[\{n_\sigma(\mathbf{r})\}\right] = K\left[\{n_\sigma(\mathbf{r})\}\right] + E_{\text{xc}}\left[\{n_\sigma(\mathbf{r})\}\right] \; . \tag{13}$$

2.2.2 Density functional, ground-state density, and ground-state energy

After the constrained search as a first step, we are led to the density functional that determines the ground-state energy and densities (Hohenberg-Kohn theorem [1])

$$\begin{aligned}
D\left[\{n_\sigma(\mathbf{r})\}\right] &= \bar{F}\left[\{n_\sigma(\mathbf{r})\}\right] + U\left[\{n_\sigma(\mathbf{r})\}\right] + V_{\text{Har}}\left[\{n_\sigma(\mathbf{r})\}\right] \\
&= K\left[\{n_\sigma(\mathbf{r})\}\right] + U\left[\{n_\sigma(\mathbf{r})\}\right] + V_{\text{Har}}\left[\{n_\sigma(\mathbf{r})\}\right] + E_{\text{xc}}\left[\{n_\sigma(\mathbf{r})\}\right]
\end{aligned} \tag{14}$$

with the ionic and Hartree energy contributions

$$\begin{aligned}
U\left[\{n_\sigma(\mathbf{r})\}\right] &= \sum_\sigma \int d\mathbf{r}\, U(\mathbf{r})\, n_\sigma(\mathbf{r}) \; , \\
V_{\text{Har}}\left[\{n_\sigma(\mathbf{r})\}\right] &= \sum_{\sigma,\sigma'} \int d\mathbf{r} \int d\mathbf{r}'\, V(\mathbf{r}-\mathbf{r}')\, n_\sigma(\mathbf{r})\, n_{\sigma'}(\mathbf{r}') \; .
\end{aligned} \tag{15}$$

According to the Ritz variational principle, the ground-state energy E_0 is found from the minimization of this functional over the densities $n_\sigma(\mathbf{r})$,

$$E_0 = \text{Min}_{\{n_\sigma(\mathbf{r})\}} D\left[\{n_\sigma(\mathbf{r})\}\right] \; . \tag{16}$$

The ground-state densities $n_\sigma^0(\mathbf{r})$ are those where the minimum of $D\left[\{n_\sigma(\mathbf{r})\}\right]$ is obtained.

2.3 Single-particle reference system

We consider the subset of single-particle product states $|\Phi^{(n)}\rangle$ that are normalized to unity, $\langle\Phi^{(n)}|\Phi^{(n)}\rangle = 1$. As before, the upper index indicates that they all lead to the same (physical) single-particle densities $n_\sigma^{\mathrm{sp}}(\mathbf{r})$,

$$n_\sigma^{\mathrm{sp}}(\mathbf{r}) = \langle\Phi^{(n)}|\hat{\Psi}_\sigma^\dagger(\mathbf{r})\hat{\Psi}_\sigma(\mathbf{r})|\Phi^{(n)}\rangle \ . \tag{17}$$

As our single-particle Hamiltonian we consider the kinetic-energy operator $\hat{H}_{\mathrm{kin}}$, see eq. (6). For fixed single-particle densities $n_\sigma^{\mathrm{sp}}(\mathbf{r})$ we define the single-particle kinetic-energy functional

$$F_{\mathrm{sp}}\left[\{n_\sigma^{\mathrm{sp}}(\mathbf{r})\},\left\{|\Phi^{(n)}\rangle\right\}\right] = \langle\Phi^{(n)}|\hat{H}_{\mathrm{kin}}|\Phi^{(n)}\rangle \ . \tag{18}$$

2.3.1 Constrained search

As in Sect. 2.2, we carry out a constrained search in the subset of states $|\Phi^{(n)}\rangle$. The task is the minimization of the kinetic-energy functional $F_{\mathrm{sp}}\left[\{n_\sigma^{\mathrm{sp}}(\mathbf{r})\},\left\{|\Phi^{(n)}\rangle\right\}\right]$. We denote the optimized single-particle product state by $|\Phi_0^{(n)}\rangle$ so that we find the density functional for the kinetic energy as

$$\bar{F}_{\mathrm{sp}}\left[\{n_\sigma^{\mathrm{sp}}(\mathbf{r})\}\right] = \langle\Phi_0^{(n)}|\hat{H}_{\mathrm{kin}}|\Phi_0^{(n)}\rangle \equiv K_{\mathrm{sp}}\left[\{n_\sigma^{\mathrm{sp}}(\mathbf{r})\}\right] \ . \tag{19}$$

2.3.2 Single-particle density functional

As the density functional $D_{\mathrm{sp}}\left[\{n_\sigma^{\mathrm{sp}}(\mathbf{r})\}\right]$ that corresponds to the single-particle problem we define

$$D_{\mathrm{sp}}\left[\{n_\sigma^{\mathrm{sp}}(\mathbf{r})\}\right] = K_{\mathrm{sp}}\left[\{n_\sigma^{\mathrm{sp}}(\mathbf{r})\}\right] + U\left[\{n_\sigma^{\mathrm{sp}}(\mathbf{r})\}\right] + V_{\mathrm{Har}}\left[\{n_\sigma^{\mathrm{sp}}(\mathbf{r})\}\right] + E_{\mathrm{sp,xc}}\left[\{n_\sigma^{\mathrm{sp}}(\mathbf{r})\}\right] \tag{20}$$

with the kinetic energy term from (19), the contributions from the external potential and the Hartree terms $U\left[\{n_\sigma^{\mathrm{sp}}(\mathbf{r})\}\right]$ and $V_{\mathrm{Har}}\left[\{n_\sigma^{\mathrm{sp}}(\mathbf{r})\}\right]$ from eq. (15), and a single-particle exchange-correlation potential $E_{\mathrm{sp,xc}}\left[\{n_\sigma^{\mathrm{sp}}(\mathbf{r})\}\right]$ that we will specify later. The functional (20) defines our single-particle reference system.

2.3.3 Noninteracting V-representability

In order to link the many-particle and single-particle approaches we make the assumption of non-interacting V-representability [1]: For any given (physical) density $n_\sigma(\mathbf{r})$ we can find a subset of normalized single-particle product states $|\Phi^{(n)}\rangle$ with N electrons such that

$$n_\sigma^{\mathrm{sp}}(\mathbf{r}) = n_\sigma(\mathbf{r}) \ . \tag{21}$$

Moreover, we demand that the density functionals $D\left[\{n_\sigma(\mathbf{r})\}\right]$ (14) for the interacting electrons and $D_{\mathrm{sp}}\left[\{n_\sigma(\mathbf{r})\}\right]$ (20) for the single-particle problem agree with each other [15],

$$D_{\mathrm{sp}}\left[\{n_\sigma(\mathbf{r})\}\right] = D\left[\{n_\sigma(\mathbf{r})\}\right] \ . \tag{22}$$

Then, the single-particle problem leads to the same ground-state density $n_\sigma^0(\mathbf{r})$ and ground-state energy E_0 as the interacting-particle Hamiltonian because the density variation is done with the same density functional (Kohn-Sham theorem) [1].

The condition (22) is equivalent to

$$K_{\mathrm{sp}}\left[\{n_\sigma(\mathbf{r})\}\right] + E_{\mathrm{sp,xc}}\left[\{n_\sigma(\mathbf{r})\}\right] = K\left[\{n_\sigma(\mathbf{r})\}\right] + E_{\mathrm{xc}}\left[\{n_\sigma(\mathbf{r})\}\right] \tag{23}$$

because the interaction with the external potential and the Hartree term only depend on the densities that are presumed equal for the interacting problem and the non-interacting reference system, see eq. (21). Eq. (23) then leads to an exact expression for the single-particle exchange-correlation energy

$$E_{\mathrm{sp,xc}}\left[\{n_\sigma(\mathbf{r})\}\right] \;=\; K\left[\{n_\sigma(\mathbf{r})\}\right] - K_{\mathrm{sp}}\left[\{n_\sigma(\mathbf{r})\}\right] + E_{\mathrm{xc}}\left[\{n_\sigma(\mathbf{r})\}\right] \; . \tag{24}$$

This is our defining equation for $E_{\mathrm{sp,xc}}\left[\{n_\sigma(\mathbf{r})\}\right]$ in eq. (20).

2.4   Kohn-Sham Hamiltonian

In the following we address the single-particle energy functional directly, i.e., the Ritz variational problem without a prior constrained search,

$$E\left[\{n_\sigma(\mathbf{r})\}, \{|\Phi\rangle\}\right] = \langle\Phi|\hat{H}_{\mathrm{kin}}|\Phi\rangle + U\left[\{n_\sigma(\mathbf{r})\}\right] + V_{\mathrm{Har}}\left[\{n_\sigma(\mathbf{r})\}\right] + E_{\mathrm{sp,xc}}\left[\{n_\sigma(\mathbf{r})\}\right] \; . \tag{25}$$

For the extension to the Gutzwiller Density Functional Theory in Sect. 3, we expand the field operators in a basis,

$$\hat{\Psi}_\sigma(\mathbf{r}) = \sum_i \langle\mathbf{r}|i,\sigma\rangle\hat{c}_{i,\sigma} \quad , \quad \hat{\Psi}_\sigma^\dagger(\mathbf{r}) = \sum_i \hat{c}_{i,\sigma}^\dagger\langle i,\sigma|\mathbf{r}\rangle \; , \tag{26}$$

where the index i represents a combination of site (or crystal momentum) index and an orbital index. For a canonical basis we must have completeness and orthogonality,

$$\sum_{i,\sigma}|i,\sigma\rangle\langle i,\sigma| = \hat{1} \quad , \quad \langle i,\sigma|j,\sigma'\rangle = \delta_{i,j}\delta_{\sigma,\sigma'} \; . \tag{27}$$

When we insert (26) into (6), we obtain the operator for the kinetic energy in a general single-particle basis,

$$\hat{H}_{\mathrm{kin}} = \sum_{i,j,\sigma} T_{i,j;\sigma}\hat{c}_{i,\sigma}^\dagger\hat{c}_{j,\sigma} \; , \tag{28}$$

where the elements of the kinetic-energy matrix $\widetilde{T}_\sigma$ are given by

$$T_{i,j;\sigma} = \int d\mathbf{r}\, \xi_{i,\sigma}^*(\mathbf{r})\left(-\frac{\Delta_{\mathbf{r}}}{2m}\right)\xi_{j,\sigma}(\mathbf{r}) \; , \tag{29}$$

with $\xi_{i,\sigma}(\mathbf{r}) = \langle\mathbf{r}|i,\sigma\rangle$.

2.4.1   Energy functional

We introduce the single-particle density matrix $\tilde{\rho}$. Its elements in the general single-particle basis read

$$\rho_{(i,\sigma),(j,\sigma)} = \langle\Phi|\hat{c}_{j,\sigma}^\dagger\hat{c}_{i,\sigma}|\Phi\rangle \equiv \rho_{i,j;\sigma} \ . \tag{30}$$

Then, the densities are given by

$$n_\sigma(\mathbf{r}) = \sum_{i,j} \xi_{i,\sigma}^*(\mathbf{r})\xi_{j,\sigma}(\mathbf{r})\rho_{j,i;\sigma} \ . \tag{31}$$

Using these definitions, we can write the energy functional in the form

$$E\left[\{n_\sigma(\mathbf{r})\},\tilde{\rho}\right] = \sum_{i,j}\sum_\sigma T_{i,j;\sigma}\rho_{j,i;\sigma} + U\left[\{n_\sigma(\mathbf{r})\}\right] + V_{\mathrm{Har}}\left[\{n_\sigma(\mathbf{r})\}\right] + E_{\mathrm{sp,xc}}\left[\{n_\sigma(\mathbf{r})\}\right] \ . \tag{32}$$

The fact that $|\Phi\rangle$ are normalized single-particle product states is encoded in the matrix relation

$$\tilde{\rho}\cdot\tilde{\rho} = \tilde{\rho} \ . \tag{33}$$

This is readily proven by using a unitary transformation between the operators $\hat{c}_{i,\sigma}$ and the single-particle operators $\hat{b}_{k,\sigma}$ that generate $|\Phi\rangle$, see appendix A.1.1.

When we minimize $E\left[\{n_\sigma(\mathbf{r})\},\tilde{\rho}\right]$ with respect to $\tilde{\rho}$ we must take the condition (33) into account using a matrix $\widetilde{\Omega}$ of Lagrange multipliers $\Omega_{l,m;\sigma}$. Moreover, we use the Lagrange multipliers $\kappa_\sigma(\mathbf{r})$ to ensure eq. (31). Altogether we address $G_{\mathrm{DFT}} \equiv G_{\mathrm{DFT}}\left[\tilde{\rho},\widetilde{\Omega},\{n_\sigma(\mathbf{r})\},\{\kappa_\sigma(\mathbf{r})\}\right]$

$$\begin{aligned}
G_{\mathrm{DFT}} \ = \ & E\left[\{n_\sigma(\mathbf{r})\},\tilde{\rho}\right] - \sum_{l,m,\sigma}\Omega_{l,m;\sigma}\left(\sum_p \rho_{l,p;\sigma}\rho_{p,m;\sigma} - \rho_{l,m;\sigma}\right) \\
& - \sum_\sigma\int\mathrm{d}\mathbf{r}\ \kappa_\sigma(\mathbf{r})\left(n_\sigma(\mathbf{r}) - \sum_{i,j}\xi_{i,\sigma}^*(\mathbf{r})\xi_{j,\sigma}(\mathbf{r})\rho_{j,i;\sigma}\right) . \tag{34}
\end{aligned}$$

2.4.2   Minimization

When we minimize G_{DFT} in eq. (34) with respect to $n_\sigma(\mathbf{r})$ we find

$$\kappa_\sigma(\mathbf{r}) \ = \ U(\mathbf{r}) + V_{\mathrm{Har}}(\mathbf{r}) + v_{\mathrm{sp,xc},\sigma}(\mathbf{r}) \ , \tag{35}$$

$$V_{\mathrm{Har}}(\mathbf{r}) \ \equiv \ \sum_{\sigma'}\int\mathrm{d}\mathbf{r}'\,2V(\mathbf{r}-\mathbf{r}')n_{\sigma'}^0(\mathbf{r}') \ , \tag{36}$$

$$\begin{aligned}
v_{\mathrm{sp,xc},\sigma}(\mathbf{r}) \ \equiv \ & \left.\frac{\partial E_{\mathrm{sp,xc}}\left[\{n_{\sigma'}(\mathbf{r}')\}\right]}{\partial n_\sigma(\mathbf{r})}\right|_{n_\sigma(\mathbf{r})=n_\sigma^0(\mathbf{r})} \\
= \ & \left.\frac{\partial\left[K\left[\{n_{\sigma'}(\mathbf{r}')\}\right] - K_{\mathrm{sp}}\left[\{n_{\sigma'}(\mathbf{r}')\}\right] + E_{\mathrm{xc}}\left[\{n_{\sigma'}(\mathbf{r}')\}\right]\right]}{\partial n_\sigma(\mathbf{r})}\right|_{n_\sigma(\mathbf{r})=n_\sigma^0(\mathbf{r})} , \tag{37}
\end{aligned}$$

where $V_{\mathrm{Har}}(\mathbf{r})$ is the Hartree interaction and $v_{\mathrm{sp,xc},\sigma}(\mathbf{r})$ is the single-particle exchange-correlation potential.

The minimization with respect to $\tilde{\rho}$ is outlined in appendix A.1.2, see also Ref. [16]. It leads to the Kohn-Sham single-particle Hamiltonian

$$\hat{H}^{\mathrm{KS}} = \sum_{i,j,\sigma} T^{\mathrm{KS}}_{i,j;\sigma} \hat{c}^{\dagger}_{i,\sigma} \hat{c}_{j,\sigma} , \tag{38}$$

where the elements of the Kohn-Sham Hamilton matrix $\widetilde{T}^{\mathrm{KS}}_{\sigma}$ are given by

$$T^{\mathrm{KS}}_{i,j;\sigma} = \frac{\partial E\left[\{n_\sigma(\mathbf{r})\}, \tilde{\rho}\right]}{\partial \rho_{j,i;\sigma}} + \int \mathrm{d}\mathbf{r}\, \kappa_\sigma(\mathbf{r}) \xi^*_{i,\sigma}(\mathbf{r}) \xi_{j,\sigma}(\mathbf{r}) . \tag{39}$$

Explicitly,

$$T^{\mathrm{KS}}_{i,j;\sigma} = \int \mathrm{d}\mathbf{r}\, \xi^*_{i,\sigma}(\mathbf{r}) h^{\mathrm{KS}}_{\sigma}(\mathbf{r}) \xi_{j,\sigma}(\mathbf{r}) , \tag{40}$$

$$h^{\mathrm{KS}}_{\sigma}(\mathbf{r}) \equiv -\frac{\Delta_{\mathbf{r}}}{2m} + V^{\mathrm{KS}}_{\sigma}(\mathbf{r}) , \tag{41}$$

$$V^{\mathrm{KS}}_{\sigma}(\mathbf{r}) \equiv \kappa_\sigma(\mathbf{r}) = U(\mathbf{r}) + V_{\mathrm{Har}}(\mathbf{r}) + v_{\mathrm{sp,xc},\sigma}(\mathbf{r}) . \tag{42}$$

Here, we defined the 'Kohn-Sham potential' $V^{\mathrm{KS}}_{\sigma}(\mathbf{r})$ that, in our derivation, is identical to the Lagrange parameter $\kappa_\sigma(\mathbf{r})$.

The remaining task is to find the basis in which the Kohn-Sham matrix $\widetilde{T}^{\mathrm{KS}}_{\sigma}$ is diagonal, for a translationally invariant system, see appendix A.1.3. This gives the dispersion $\varepsilon_{\mathrm{n}}(\mathbf{k})$ of the Kohn-Sham quasi-particles.

3 DFT for many-particle reference systems

The Kohn-Sham potential (37) cannot be calculated exactly because the functionals in eq. (24) are not known. Therefore, assumptions must be made about the form of the single-particle exchange-correlation potential, e.g., the Local Density Approximation [1]. Unfortunately, such approximations are often not satisfactory, e.g., for transition metals. Consequently, more sophisticated many-electron approaches must be employed to improve the Kohn-Sham approach.

3.1 Hubbard Hamiltonian and Hubbard density functional

3.1.1 Multi-band Hubbard model

A better description of transition metals and their compounds can be achieved by supplementing the single-particle reference system resulting from $\hat{H}_{\mathrm{kin}}$ in Sect. 2.3 by a multi-band Hubbard interaction. Then, our multi-band reference system follows from

$$\hat{H}_{\mathrm{H}} = \hat{H}_{\mathrm{kin}} + \hat{V}_{\mathrm{loc}} - \hat{V}_{\mathrm{dc}} , \tag{43}$$

where $\hat{V}_{\mathrm{loc}}$ describes local interactions between electrons in Wannier orbitals on the same site $\mathbf{R}$. The local single-particle operator $\hat{V}_{\mathrm{dc}}$ accounts for the double counting of their interactions in

the Hubbard term $\hat{V}_{\mathrm{loc}}$ and in the single-particle exchange-correlation energy $E_{\mathrm{sp,xc}}$. We assume that $\hat{V}_{\mathrm{loc}}$ and $\hat{V}_{\mathrm{dc}}$ do not depend on the densities $n_\sigma(\mathbf{r})$ explicitly.

For the local interaction we set

$$
\begin{aligned}
\hat{V}_{\mathrm{loc}} &= \sum_{\mathbf{R}} \hat{V}_{\mathrm{loc}}(\mathbf{R}) \,, \\
\hat{V}_{\mathrm{loc}}(\mathbf{R}) &= \frac{1}{2} \sum_{(c_1,\sigma_1),\ldots,(c_4,\sigma_4)} U^{(c_1,\sigma_1),(c_2,\sigma_2)}_{(c_3,\sigma_3),(c_4,\sigma_4)} \hat{c}^{\dagger}_{\mathbf{R},c_1,\sigma_1} \hat{c}^{\dagger}_{\mathbf{R},c_2,\sigma_2} \hat{c}_{\mathbf{R},c_3,\sigma_3} \hat{c}_{\mathbf{R},c_4,\sigma_4} \,.
\end{aligned}
\tag{44}
$$

Note that only electrons in the small subset of correlated orbitals (index c) experience the two-particle interaction $\hat{V}_{\mathrm{loc}}$: When there are two electrons in the Wannier orbitals $\phi_{\mathbf{R},c_3,\sigma_3}(\mathbf{r})$ and $\phi_{\mathbf{R},c_4,\sigma_4}(\mathbf{r})$ centered around the lattice site $\mathbf{R}$, they are scattered into the orbitals $\phi_{\mathbf{R},c_1,\sigma_1}(\mathbf{r})$ and $\phi_{\mathbf{R},c_2,\sigma_2}(\mathbf{r})$, centered around the same lattice site $\mathbf{R}$; for the definition of basis states, see appendix A.1.3. Typically, we consider $c = 3d$ for the transition metals and their compounds. The interaction strengths are parameters of the theory; for a comprehensive symmetry analysis, see Ref. [17]. Later, we shall employ the spherical approximation so that $U^{...}_{...}$ for d-electrons can be expressed in terms of three Racah parameters A, B, and C. Fixing C/B makes it possible to introduce an effective Hubbard parameter U and an effective Hund's-rule coupling J, see Sect. 3.4 and appendix A.2. Due to screening, the effective Hubbard interaction U is smaller than its bare, atomic value. In general, U and J are chosen to obtain good agreement with experiment, see Sect. 4.

3.1.2 Hubbard density functional

According to Levy's constrained search, we must find the minimum of the functional

$$
F_{\mathrm{H}} \left[\{n_\sigma(\mathbf{r})\}, \{|\Psi^{(n)}\rangle\} \right] = \langle \Psi^{(n)} | \hat{H}_{\mathrm{H}} | \Psi^{(n)} \rangle
\tag{45}
$$

in the subset of normalized states with given (physical) density $n_\sigma(\mathbf{r})$, see eq. (4). The minimum of $F_{\mathrm{H}} \left[\{n_\sigma(\mathbf{r})\}, \{|\Psi^{(n)}\rangle\} \right]$ over the states $|\Psi^{(n)}\rangle$ is the ground state $|\Psi^{(n)}_{\mathrm{H},0}\rangle$ of the Hamiltonian $\hat{H}_{\mathrm{H}}$ for fixed densities $n_\sigma(\mathbf{r})$. In analogy to Sect. 2.3, we define the Hubbard density functional

$$
\begin{aligned}
D_{\mathrm{H}} \left[\{n_\sigma(\mathbf{r})\} \right] = {} & K_{\mathrm{H}} \left[\{n_\sigma(\mathbf{r})\} \right] + U \left[\{n_\sigma(\mathbf{r})\} \right] + V_{\mathrm{Har}} \left[\{n_\sigma(\mathbf{r})\} \right] \\
& + V_{\mathrm{loc}} \left[\{n_\sigma(\mathbf{r})\} \right] - V_{\mathrm{dc}} \left[\{n_\sigma(\mathbf{r})\} \right] + E_{\mathrm{H,xc}} \left[\{n_\sigma(\mathbf{r})\} \right] \,,
\end{aligned}
\tag{46}
$$

where

$$
K_{\mathrm{H}} \left[\{n_\sigma(\mathbf{r})\} \right] = \langle \Psi^{(n)}_{\mathrm{H},0} | \hat{H}_{\mathrm{kin}} | \Psi^{(n)}_{\mathrm{H},0} \rangle \,, \quad V_{\mathrm{loc/dc}} \left[\{n_\sigma(\mathbf{r})\} \right] = \langle \Psi^{(n)}_{\mathrm{H},0} | \hat{V}_{\mathrm{loc/dc}} | \Psi^{(n)}_{\mathrm{H},0} \rangle \,,
\tag{47}
$$

and $E_{\mathrm{H,xc}} \left[\{n_\sigma(\mathbf{r})\} \right]$ is the exchange-correlation energy for $\hat{H}_{\mathrm{H}}$. As in Sect. 2.3, the Hubbard density functional agrees with the exact density functional if we choose

$$
\begin{aligned}
E_{\mathrm{H,xc}} \left[\{n_\sigma(\mathbf{r})\} \right] = {} & K \left[\{n_\sigma(\mathbf{r})\} \right] - K_{\mathrm{H}} \left[\{n_\sigma(\mathbf{r})\} \right] + E_{\mathrm{xc}} \left[\{n_\sigma(\mathbf{r})\} \right] \\
& - \left(V_{\mathrm{loc}} \left[\{n_\sigma(\mathbf{r})\} \right] - V_{\mathrm{dc}} \left[\{n_\sigma(\mathbf{r})\} \right] \right) \,.
\end{aligned}
\tag{48}
$$

Then, the Hubbard approach provides the exact ground-state densities and ground-state energy of our full many-particle Hamiltonian (Hohenberg-Kohn–Hubbard theorem). Of course, our derivation relies on the assumption of Hubbard V-representability of the densities $n_\sigma(\mathbf{r})$.

3.1.3 Hubbard single-particle potential

When we directly apply Ritz' principle, we have to minimize the energy functional

$$E\left[\{n_\sigma(\mathbf{r})\},\{|\Psi\rangle\}\right] = \langle\Psi|\hat{H}_{\mathrm{H}}|\Psi\rangle + U\left[\{n_\sigma(\mathbf{r})\}\right] + V_{\mathrm{Har}}\left[\{n_\sigma(\mathbf{r})\}\right] + E_{\mathrm{H,xc}}\left[\{n_\sigma(\mathbf{r})\}\right]. \quad (49)$$

We include the constraints eq. (4) and the normalization condition using the Lagrange parameters $\kappa_\sigma(\mathbf{r})$ and E_0 in the functional $G_{\mathrm{H}} \equiv G_{\mathrm{H}}\left[\{|\Psi\rangle\},\{n_\sigma(\mathbf{r})\},\{\kappa_\sigma(\mathbf{r})\},E_0\right]$

$$G_{\mathrm{H}} = E\left[\{n_\sigma(\mathbf{r})\},\{|\Psi\rangle\}\right] - E_0\left(\langle\Psi|\Psi\rangle - 1\right) - \sum_\sigma\int\mathrm{d}\mathbf{r}\,\kappa_\sigma(\mathbf{r})\left(n_\sigma(\mathbf{r}) - \langle\Psi|\hat{\Psi}_\sigma^\dagger(\mathbf{r})\hat{\Psi}_\sigma(\mathbf{r})|\Psi\rangle\right). \quad (50)$$

As in Sect. 2.4, see eqs. (35) and (42), the variation of G_{H} with respect to $n_\sigma(\mathbf{r})$ gives the single-particle potential

$$\begin{aligned}
V_\sigma^{\mathrm{H}}(\mathbf{r}) &\equiv U(\mathbf{r}) + V_{\mathrm{Har}}(\mathbf{r}) + v_{\mathrm{H,xc},\sigma}(\mathbf{r}), \\
v_{\mathrm{H,xc},\sigma}(\mathbf{r}) &\equiv \left.\frac{\partial E_{\mathrm{H,xc}}\left[\{n_{\sigma'}(\mathbf{r}')\}\right]}{\partial n_\sigma(\mathbf{r})}\right|_{n_\sigma(\mathbf{r})=n_\sigma^0(\mathbf{r})}.
\end{aligned} \quad (51)$$

The Hubbard-model approach is based on the idea that typical approximations for the exchange-correlation energy, e.g., the local-density approximation, are better suited for the Hubbard model than for the Kohn-Sham approach,

$$E_{\mathrm{H,xc}}\left[\{n_\sigma(\mathbf{r})\}\right] \approx E_{\mathrm{LDA,xc}}\left[\{n_\sigma(\mathbf{r})\}\right]. \quad (52)$$

Indeed, as seen from eq. (48), in the Hubbard exchange-correlation energy $E_{\mathrm{H,xc}}$ the exchange-correlation contributions in the exact E_{xc} are reduced by the Hubbard term $V_{\mathrm{loc}}\left[\{n_\sigma(\mathbf{r})\}\right] - V_{\mathrm{dc}}\left[\{n_\sigma(\mathbf{r})\}\right]$, reflecting a more elaborate treatment of local correlations.

Unfortunately, the minimization of (49) with respect to $|\Psi\rangle$ constitutes an unsolvable many-particle problem. Indeed, the ground state $|\Psi_0\rangle$ is the solution of the many-particle Schrödinger equation with energy E_0,

$$\left(\hat{H}_0 + \hat{V}_{\mathrm{loc}} - \hat{V}_{\mathrm{dc}}\right)|\Psi_0\rangle = E_0|\Psi_0\rangle \quad (53)$$

with the single-particle Hamiltonian

$$\hat{H}_0 = \sum_\sigma\int\mathrm{d}\mathbf{r}\,\hat{\Psi}_\sigma^\dagger(\mathbf{r})\left(-\frac{\Delta_\mathbf{r}}{2m} + U(\mathbf{r}) + V_{\mathrm{Har}}(\mathbf{r}) + v_{\mathrm{H,xc},\sigma}(\mathbf{r})\right)\hat{\Psi}_\sigma(\mathbf{r}). \quad (54)$$

The 'Kohn-Sham–Hubbard equations' (53) can be used as starting point for further approximations, for example, the Dynamical Mean-Field Theory (DMFT). In the following we will address the functional in eq. (49) directly.

3.2 Gutzwiller density functional

In the widely used LDA+U approach [5], the functional in eq. (49) is evaluated and (approximately) minimized by means of single-particle product wave functions. However, this approach treats correlations only on a mean-field level. In the more sophisticated Gutzwiller approach, we consider the functional in eq. (49) in the subset of Gutzwiller-correlated variational many-particle states.

3.2.1 Gutzwiller variational ground state

In order to formulate the Gutzwiller variational ground state [4,8], we consider the atomic states $|\Gamma\rangle_{\mathbf{R}}$ that are built from the correlated orbitals. The local Hamiltonians take the form

$$\hat{V}_{\text{loc/dc}}(\mathbf{R}) = \sum_{\Gamma,\Gamma'} E_{\Gamma,\Gamma'}^{\text{loc/dc}}(\mathbf{R})|\Gamma\rangle_{\mathbf{R}\mathbf{R}}\langle\Gamma'| = \sum_{\Gamma,\Gamma'} E_{\Gamma,\Gamma'}^{\text{loc/dc}}(\mathbf{R})\hat{m}_{\mathbf{R};\Gamma,\Gamma'} \;, \tag{55}$$

where $|\Gamma\rangle_{\mathbf{R}}$ contains $|\Gamma_{\mathbf{R}}|$ electrons. Here, we introduced

$$E_{\Gamma,\Gamma'}^{\text{loc/dc}}(\mathbf{R}) = {}_{\mathbf{R}}\langle\Gamma|\hat{V}_{\text{loc/dc}}(\mathbf{R})|\Gamma'\rangle_{\mathbf{R}} \tag{56}$$

and the local many-particle operators $\hat{m}_{\mathbf{R};\Gamma,\Gamma'} = |\Gamma\rangle_{\mathbf{R}\mathbf{R}}\langle\Gamma'|$.
The Gutzwiller correlator and the Gutzwiller variational states are defined as

$$\hat{P}_{\text{G}} = \prod_{\mathbf{R}} \sum_{\Gamma,\Gamma'} \lambda_{\Gamma,\Gamma'}(\mathbf{R})\hat{m}_{\mathbf{R};\Gamma,\Gamma'} \quad,\quad |\Psi_{\text{G}}\rangle = \hat{P}_{\text{G}}|\Phi\rangle \;. \tag{57}$$

Here, $|\Phi\rangle$ is a single-particle product state, and $\lambda_{\Gamma,\Gamma'}(\mathbf{R})$ defines the matrix $\tilde{\lambda}(\mathbf{R})$ of, in general, complex variational parameters.

3.2.2 Gutzwiller functionals

We evaluate the energy functional (49) in the restricted subset of Gutzwiller variational states,

$$
\begin{aligned}
E\left[\{n_\sigma(\mathbf{r})\}, \{|\Psi_{\text{G}}\rangle\}\right] &= \sum_{\mathbf{R},b,\mathbf{R}',b',\sigma} T_{(\mathbf{R},b),(\mathbf{R}',b');\sigma}\rho^{\text{G}}_{(\mathbf{R}',b'),(\mathbf{R},b);\sigma} + V_{\text{loc}}^{\text{G}} - V_{\text{dc}}^{\text{G}} \\
&\quad + U\left[\{n_\sigma(\mathbf{r})\}\right] + V_{\text{Har}}\left[\{n_\sigma(\mathbf{r})\}\right] + E_{\text{H,xc}}\left[\{n_\sigma(\mathbf{r})\}\right], \\
V_{\text{loc/dc}}^{\text{G}} &= \sum_{\mathbf{R}} \sum_{\Gamma,\Gamma'} E_{\Gamma,\Gamma'}^{\text{loc/dc}}(\mathbf{R})m_{\mathbf{R};\Gamma,\Gamma'}^{\text{G}} \;.
\end{aligned} \tag{58}
$$

Note that we work with the orbital Wannier basis, see appendix A.1.3,

$$T_{(\mathbf{R},b),(\mathbf{R}',b');\sigma} = \int d\mathbf{r}\, \phi^*_{\mathbf{R},b,\sigma}(\mathbf{r})\left(-\frac{\Delta_{\mathbf{r}}}{2m}\right)\phi_{\mathbf{R}',b',\sigma}(\mathbf{r}) \;. \tag{59}$$

The elements of the Gutzwiller-correlated single-particle density matrix are

$$\rho^{\text{G}}_{(\mathbf{R}',b'),(\mathbf{R},b);\sigma} = \frac{\langle\Psi_{\text{G}}|\hat{c}^{\dagger}_{\mathbf{R},b,\sigma}\hat{c}_{\mathbf{R}',b',\sigma}|\Psi_{\text{G}}\rangle}{\langle\Psi_{\text{G}}|\Psi_{\text{G}}\rangle} = \frac{\langle\Phi|\hat{P}_{\text{G}}^{\dagger}\hat{c}^{\dagger}_{\mathbf{R},b,\sigma}\hat{c}_{\mathbf{R}',b',\sigma}\hat{P}_{\text{G}}|\Phi\rangle}{\langle\Phi|\hat{P}_{\text{G}}^{\dagger}\hat{P}_{\text{G}}|\Phi\rangle} \;, \tag{60}$$

and the densities become

$$n_\sigma(\mathbf{r}) = \sum_{\mathbf{R},b,\mathbf{R}',b'} \phi^*_{\mathbf{R},b,\sigma}(\mathbf{r})\phi_{\mathbf{R}',b',\sigma}(\mathbf{r})\rho^{\text{G}}_{(\mathbf{R}',b'),(\mathbf{R},b);\sigma} \;. \tag{61}$$

The expectation values for the atomic operators are given by

$$m_{\mathbf{R};\Gamma,\Gamma'}^{\text{G}} = \frac{\langle\Psi_{\text{G}}|\hat{m}_{\mathbf{R};\Gamma,\Gamma'}|\Psi_{\text{G}}\rangle}{\langle\Psi_{\text{G}}|\Psi_{\text{G}}\rangle} = \frac{\langle\Phi|\hat{P}_{\text{G}}^{\dagger}\hat{m}_{\mathbf{R};\Gamma,\Gamma'}\hat{P}_{\text{G}}|\Phi\rangle}{\langle\Phi|\hat{P}_{\text{G}}^{\dagger}\hat{P}_{\text{G}}|\Phi\rangle} \;. \tag{62}$$

The diagrammatic evaluation of $\rho^{\text{G}}_{(\mathbf{R}',b'),(\mathbf{R},b);\sigma}$ and of $m^{\text{G}}_{\mathbf{R};\Gamma,\Gamma'}$ shows that these quantities are functionals of the non-interacting single-particle density matrices $\tilde{\rho}$, see eq. (30), and of the variational parameters $\lambda_{\Gamma,\Gamma'}(\mathbf{R})$. Moreover, it turns out that the local, non-interacting single-particle density matrix $\tilde{C}(\mathbf{R})$ with the elements

$$C_{b,b';\sigma}(\mathbf{R}) \equiv \rho_{(\mathbf{R},b),(\mathbf{R},b');\sigma} \tag{63}$$

plays a prominent role in the Gutzwiller energy functional, in particular, for infinite lattice coordination number. Therefore, we may write

$$E\left[\{n_\sigma(\mathbf{r})\}, \{|\Psi_{\text{G}}\rangle\}\right] \equiv E^{\text{G}}\left[\tilde{\rho}, \left\{\tilde{\lambda}(\mathbf{R})\right\}, \{n_\sigma(\mathbf{r})\}, \left\{\tilde{C}(\mathbf{R})\right\}\right] . \tag{64}$$

In the Lagrange functional we shall impose the relation (63) with the help of the Hermitian Lagrange parameter matrix $\tilde{\eta}$ with entries $\eta_{(\mathbf{R},b),(\mathbf{R},b');\sigma}$. Lastly, for the analytical evaluation of eq. (64) it is helpful to impose a set of (real-valued) local constraints ($l = 1, 2, \ldots, N_{\text{con}}$)

$$g_{l,\mathbf{R}}\left[\tilde{\lambda}(\mathbf{R}), \tilde{C}(\mathbf{R})\right] = 0 , \tag{65}$$

which we implement with real Lagrange parameters $\Lambda_l(\mathbf{R})$; explicit expressions are given in eqs. (74) and (75).

In the following, we abbreviate $i = (\mathbf{R}, b)$ and $j = (\mathbf{R}', b')$. Consequently, in analogy with Sect. 2.4, we address

$$G^{\text{G}}_{\text{DFT}} \equiv G^{\text{G}}_{\text{DFT}}\begin{bmatrix} \tilde{\rho}, \{n_\sigma(\mathbf{r})\}, \left\{\tilde{C}(\mathbf{R})\right\}, \left\{\tilde{\lambda}(\mathbf{R})\right\} \\ \tilde{\Omega}, \{\kappa_\sigma(\mathbf{r})\}, \{\tilde{\eta}(\mathbf{R})\}, \{\Lambda_l(\mathbf{R})\} \end{bmatrix} \tag{66}$$

as our Lagrange functional,

$$\begin{aligned} G^{\text{G}}_{\text{DFT}} &= E^{\text{G}}\left[\tilde{\rho}, \left\{\tilde{\lambda}(\mathbf{R})\right\}, \{n_\sigma(\mathbf{r})\}, \left\{\tilde{C}(\mathbf{R})\right\}\right] - \sum_{l,m,\sigma} \Omega_{l,m;\sigma}\left(\tilde{\rho}\cdot\tilde{\rho} - \tilde{\rho}\right)_{m,l;\sigma} \\ &\quad - \sum_\sigma \int d\mathbf{r}\, \kappa_\sigma(\mathbf{r})\left(n_\sigma(\mathbf{r}) - \sum_{i,j}\phi^*_{i,\sigma}(\mathbf{r})\phi_{j,\sigma}(\mathbf{r})\rho^{\text{G}}_{j,i;\sigma}\right) \\ &\quad + \sum_{l,\mathbf{R}} \Lambda_l(\mathbf{R})g_{l,\mathbf{R}} - \sum_{\mathbf{R},b,b',\sigma} \eta_{b,b';\sigma}(\mathbf{R})\left(C_{b',b;\sigma}(\mathbf{R}) - \rho_{(\mathbf{R},b'),(\mathbf{R},b);\sigma}\right) , \end{aligned} \tag{67}$$

cf. eq. (34). Here, we took the condition (61) into account using Lagrange parameters $\kappa_\sigma(\mathbf{r})$ because the external potential, the Hartree term and the exchange-correlation potential in eq. (58) depend on the densities.

3.2.3 Minimization of the Gutzwiller energy functional

The functional $G^{\text{G}}_{\text{DFT}}$ in eq. (67) has to be minimized with respect to $n_\sigma(\mathbf{r})$, $\tilde{C}(\mathbf{R})$, $\tilde{\lambda}(\mathbf{R})$, and $\tilde{\rho}$. The variation with respect to the Lagrange parameters $\kappa_\sigma(\mathbf{r})$, $\tilde{\eta}(\mathbf{R})$, $\Lambda_l(\mathbf{R})$, and $\tilde{\Omega}$ gives the constraints (61), (63), (65), and (33), respectively.

1. As in the derivation of the exact Schrödinger equation (53), the variation of $G_{\mathrm{DFT}}^{\mathrm{G}}$ with respect to $n_\sigma(\mathbf{r})$ generates the single-particle potential,

$$\kappa_\sigma(\mathbf{r}) = V_\sigma^{\mathrm{H}}(\mathbf{r}) , \tag{68}$$

see eqs. (42) and (51).

2. The minimization with respect to $\tilde{C}(\mathbf{R})$ gives

$$\eta_{b,b';\sigma}(\mathbf{R}) = \frac{\partial E^{\mathrm{G}}}{\partial C_{b',b;\sigma}(\mathbf{R})} + \sum_l \Lambda_l(\mathbf{R}) \frac{\partial g_{l,\mathbf{R}}}{\partial C_{b',b;\sigma}(\mathbf{R})}$$
$$+ \sum_{i,j,\sigma'} \int d\mathbf{r} \, V_{\sigma'}^{\mathrm{H}}(\mathbf{r}) \phi_{i,\sigma'}^*(\mathbf{r}) \phi_{j,\sigma'}(\mathbf{r}) \frac{\partial \rho_{j,i;\sigma'}^{\mathrm{G}}}{\partial C_{b',b;\sigma}(\mathbf{R})} . \tag{69}$$

3. The minimization with respect to the Gutzwiller correlation parameters $\tilde{\lambda}(\mathbf{R})$ results in

$$0 = \frac{\partial E^{\mathrm{G}}}{\partial \lambda_{\Gamma,\Gamma'}(\mathbf{R})} + \sum_{l,m,\sigma} \int d\mathbf{r} \, V_\sigma^{\mathrm{H}}(\mathbf{r}) \phi_{l,\sigma}^*(\mathbf{r}) \phi_{m,\sigma}(\mathbf{r}) \frac{\partial \rho_{m,l,\sigma}^{\mathrm{G}}}{\partial \lambda_{\Gamma,\Gamma'}(\mathbf{R})}$$
$$+ \sum_l \Lambda_l(\mathbf{R}) \frac{\partial g_{l,\mathbf{R}}}{\partial \lambda_{\Gamma,\Gamma'}(\mathbf{R})}$$
$$= \sum_{l,m,\sigma} h_{l,m;\sigma}^0 \frac{\partial \rho_{m,l,\sigma}^{\mathrm{G}}}{\partial \lambda_{\Gamma,\Gamma'}(\mathbf{R})} + \frac{\partial \left(V_{\mathrm{loc}}^{\mathrm{G}} - V_{\mathrm{dc}}^{\mathrm{G}} \right)}{\partial \lambda_{\Gamma,\Gamma'}(\mathbf{R})} + \sum_l \Lambda_l(\mathbf{R}) \frac{\partial g_{l,\mathbf{R}}}{\partial \lambda_{\Gamma,\Gamma'}(\mathbf{R})} , \tag{70}$$

$$h_{l,m;\sigma}^0 \equiv \int d\mathbf{r} \, \phi_{l,\sigma}^*(\mathbf{r}) \left(-\frac{\Delta_{\mathbf{r}}}{2m} + U(\mathbf{r}) + V_{\mathrm{Har}}(\mathbf{r}) + v_{\mathrm{H,xc},\sigma}(\mathbf{r}) \right) \phi_{m,\sigma}(\mathbf{r}) \tag{71}$$

for all $\lambda_{\Gamma,\Gamma'}(\mathbf{R})$. Note that, in the case of complex Gutzwiller parameters, we also have to minimize with respect to $(\lambda_{\Gamma,\Gamma'}(\mathbf{R}))^*$. Using these equations we calculate the Lagrange parameters $\Lambda_l(\mathbf{R})$ that are needed in eq. (69).

4. The minimization of $G_{\mathrm{DFT}}^{\mathrm{G}}$ with respect to $\tilde{\rho}$ generates the Landau–Gutzwiller quasi-particle Hamiltonian, see appendix A.1.2,

$$\hat{H}_{\mathrm{qp}}^{\mathrm{G}} = \sum_{i,j,\sigma} h_{i,j;\sigma}^{\mathrm{G}} \hat{c}_{i,\sigma}^\dagger \hat{c}_{j,\sigma} \tag{72}$$

with the entries

$$h_{i,j;\sigma}^{\mathrm{G}} = \frac{\partial E^{\mathrm{G}}}{\partial \rho_{j,i;\sigma}} + \sum_{l,m,\sigma'} \int d\mathbf{r} \, V_{\sigma'}^{\mathrm{H}}(\mathbf{r}) \phi_{l,\sigma'}^*(\mathbf{r}) \phi_{m,\sigma'}(\mathbf{r}) \frac{\partial \rho_{m,l,\sigma'}^{\mathrm{G}}}{\partial \rho_{j,i;\sigma}} + \sum_{\mathbf{R},b,b',\sigma'} \eta_{b,b';\sigma'}(\mathbf{R}) \frac{\partial \rho_{(\mathbf{R},b'),(\mathbf{R},b);\sigma'}}{\partial \rho_{j,i;\sigma}}$$
$$= \sum_{l,m,\sigma'} h_{l,m;\sigma'}^0 \frac{\partial \rho_{m,l,\sigma'}^{\mathrm{G}}}{\partial \rho_{j,i;\sigma}} + \frac{\partial \left(V_{\mathrm{loc}}^{\mathrm{G}} - V_{\mathrm{dc}}^{\mathrm{G}} \right)}{\partial \rho_{j,i;\sigma}} + \sum_{\mathbf{R},b,b'} \delta_{j,(\mathbf{R},b')} \delta_{i,(\mathbf{R},b)} \eta_{b,b';\sigma}(\mathbf{R}), \tag{73}$$

where we used eqs. (58) and (71).

The single-particle state $|\Phi\rangle$ is the ground state of the Hamiltonian (72) from which the single-particle density matrix $\tilde{\rho}$ follows.

The minimization problem outlined in steps (i)–(iv) requires the evaluation of the energy E^{G} in eq. (58). In particular, the correlated single-particle density matrix $\tilde{\rho}^{\mathrm{G}}$, eq. (60), must be determined.

All equations derived in this section are completely general. They can, at least in principle, be evaluated by means of a diagrammatic expansion method [18–21]. The leading order of the expansion corresponds to an approximation-free evaluation of expectation values for Gutzwiller wave functions in the limit of large lattice coordination number. This limit, also known as "Gutzwiller Approximation", will be studied in the rest of this chapter.

3.3   Gutzwiller density functional for infinite lattice coordination number

For $Z \to \infty$, the Gutzwiller-correlated single-particle density matrix and the Gutzwiller probabilities for the local occupancies can be calculated explicitly without further approximations; for a formal proof, see Ref. [21]. In this section we make no symmetry assumptions (translational invariance, crystal symmetries). Note, however, that the equations do not cover the case of spin-orbit coupling; for the latter, see Refs. [22, 23].

3.3.1   Local constraints

As shown in Refs. [8, 24] it is convenient for the evaluation of Gutzwiller wave functions to impose the following (local) constraints

$$\sum_{\Gamma,\Gamma_1,\Gamma_2} \lambda^*_{\Gamma,\Gamma_1}(\mathbf{R})\lambda_{\Gamma,\Gamma_2}(\mathbf{R})\langle \hat{m}_{\mathbf{R};\Gamma_1,\Gamma_2}\rangle_\Phi = 1 \tag{74}$$

and

$$\sum_{\Gamma,\Gamma_1,\Gamma_2} \lambda^*_{\Gamma,\Gamma_1}(\mathbf{R})\lambda_{\Gamma,\Gamma_2}(\mathbf{R})\langle \hat{m}_{\mathbf{R};\Gamma_1,\Gamma_2}\hat{c}^\dagger_{\mathbf{R},b,\sigma}\hat{c}_{\mathbf{R},b',\sigma}\rangle_\Phi = \langle \hat{c}^\dagger_{\mathbf{R},b,\sigma}\hat{c}_{\mathbf{R},b',\sigma}\rangle_\Phi \,, \tag{75}$$

where we abbreviated $\langle \hat{A}\rangle_\Phi \equiv \langle \Phi|\hat{A}|\Phi\rangle$. Note that, for complex constraints, the index l in (65) labels real and imaginary parts separately.

3.3.2   Atomic occupancies

In the limit of infinite lattice coordination number, the interaction and double-counting energy can be expressed solely in terms of the local variational parameters $\tilde{\lambda}(\mathbf{R})$ and the local density matrix $\tilde{C}(\mathbf{R})$ of the correlated bands in $|\Phi\rangle$,

$$V^{\mathrm{G}}_{\mathrm{loc/dc}} = \sum_{\mathbf{R}} \sum_{\Gamma_1,\ldots,\Gamma_4} \lambda^*_{\Gamma_2,\Gamma_1}(\mathbf{R}) E^{\mathrm{loc/dc}}_{\Gamma_2,\Gamma_3}(\mathbf{R})\lambda_{\Gamma_3,\Gamma_4}(\mathbf{R})\langle \hat{m}_{\mathbf{R};\Gamma_1,\Gamma_4}\rangle_\Phi \,. \tag{76}$$

The remaining expectation values $\langle \hat{m}_{\mathbf{R};\Gamma_1,\Gamma_4}\rangle_\Phi$ are evaluated using Wick's theorem. Explicit expressions are given in Refs. [8, 25].

3.3.3   Correlated single-particle density matrix

The local part of the correlated single-particle density matrix is given by

$$\rho^{\mathrm{G}}_{(\mathbf{R},b'),(\mathbf{R},b);\sigma} = \sum_{\Gamma_1,\ldots,\Gamma_4} \lambda^*_{\Gamma_2,\Gamma_1}(\mathbf{R})\lambda_{\Gamma_3,\Gamma_4}(\mathbf{R})\langle \hat{m}_{\mathbf{R};\Gamma_1,\Gamma_2}\hat{c}^\dagger_{\mathbf{R},b,\sigma}\hat{c}_{\mathbf{R},b',\sigma}\hat{m}_{\mathbf{R};\Gamma_3,\Gamma_4}\rangle_{\Phi} \equiv C^{\mathrm{G}}_{b',b;\sigma}(\mathbf{R}). \quad (77)$$

It can be evaluated using Wick's theorem. As can be seen from eq. (77), it is a function of the variational parameters $\lambda_{\Gamma,\Gamma'}(\mathbf{R})$ and of the local non-interacting single-particle density matrix $\tilde{C}(\mathbf{R})$.

For $\mathbf{R} \neq \mathbf{R}'$, we have for the correlated single-particle density matrix

$$\rho^{\mathrm{G}}_{(\mathbf{R}',b'),(\mathbf{R},b);\sigma} = \sum_{a,a'} q^{a,\sigma}_{b,\sigma}(\mathbf{R})\left(q^{a',\sigma}_{b',\sigma}(\mathbf{R}')\right)^* \rho_{(\mathbf{R}',a'),(\mathbf{R},a);\sigma} \quad (78)$$

with the orbital-dependent renormalization factors $q^{a;\sigma}_{b,\sigma}(\mathbf{R})$ for the electron transfer between different sites. Explicit expressions in terms of the variational parameters $\tilde{\lambda}(\mathbf{R})$ and of the local non-interacting single-particle density matrix $\tilde{C}(\mathbf{R})$ are given in Refs. [8, 25].

3.3.4   Implementation for translational invariant systems

For a system that is invariant under translation by a lattice vector and contains only one atom per unit cell, all local quantities become independent of the site index, e.g., $\lambda_{\Gamma,\Gamma'}(\mathbf{R}) \equiv \lambda_{\Gamma,\Gamma'}$ for the Gutzwiller variational parameters. Since $\mathbf{k}$ from the first Brillouin zone is a good quantum number, we work with the (orbital) Bloch basis, see appendix A.1.3.

The minimization of the energy functional with respect to the single-particle density matrix leads to the Gutzwiller–Kohn-Sham Hamiltonian. In the orbital Bloch basis $\phi_{\mathbf{k},b,\sigma}(\mathbf{r})$, see appendix A.1.3, the corresponding quasi-particle Hamiltonian reads,

$$\hat{H}^{\mathrm{G}}_{\mathrm{qp}} = \sum_{\mathbf{k},b,b',\sigma} h^{\mathrm{G}}_{b,b';\sigma}(\mathbf{k})\hat{c}^\dagger_{\mathbf{k},b,\sigma}\hat{c}_{\mathbf{k},b',\sigma} \, , \quad (79)$$

see eq. (72). The Landau-Gutzwiller quasi-particle dispersion $\varepsilon^{\mathrm{G}}_{n,\sigma}(\mathbf{k})$ follows from the diagonalization of $h^{\mathrm{G}}_{b,b';\sigma}(\mathbf{k})$. For explicit expressions for $h^{\mathrm{G}}_{b,b';\sigma}(\mathbf{k})$ and the actual numerical implementation within QUANTUMESPRESSO, see Refs. [12, 13].

3.4   Local Hamiltonian and double counting for transition metals

For a Gutzwiller DFT calculation we need to specify the Coulomb parameters in the local Hamiltonian and the form of the double-counting operator in eqs. (43) and (44).

3.4.1   Cubic symmetry and spherical approximation

In many theoretical studies one uses a local Hamiltonian with only density-density interactions,

$$\hat{V}^{\mathrm{dens}}_{\mathrm{loc}} = \frac{1}{2}\sum_{c,\sigma} U(c,c)\hat{n}_{c,\sigma}\hat{n}_{c,\bar{\sigma}} + \frac{1}{2}\sum_{c(\neq)c'}\sum_{\sigma,\sigma'} \widetilde{U}_{\sigma,\sigma'}(c,c')\hat{n}_{c,\sigma}\hat{n}_{c',\sigma'} \, . \quad (80)$$

Here, we introduced $\bar{\uparrow} = \downarrow$ ($\bar{\downarrow} = \uparrow$) and $\widetilde{U}_{\sigma,\sigma'}(c,c') = U(c,c') - \delta_{\sigma,\sigma'}J(c,c')$, where $U(c,c')$ and $J(c,c')$ are the local Hubbard and Hund's-rule exchange interactions. An additional and quite common approximation is the use of orbital-independent Coulomb parameters,

$$U(c,c) \equiv U, \quad \text{and} \quad U(c,c') \equiv U', \ J(c,c') \equiv J \quad \text{for } c \neq c'. \tag{81}$$

For a system of five correlated $3d$ orbitals in a cubic environment as in nickel and iron, however, the Hamiltonian (80) is incomplete [26]. The full Hamiltonian reads

$$\hat{V}_{\text{loc}}^{\text{full}} = \hat{V}_{\text{loc}}^{\text{dens}} + \hat{V}_{\text{loc}}^{\text{n.dens.}}, \tag{82}$$

where

$$
\begin{aligned}
\hat{V}_{\text{loc}}^{\text{n.dens.}} &= \frac{1}{2}\sum_{c(\neq)c'} J(c,c')\left(\hat{c}_{c,\uparrow}^{\dagger}\hat{c}_{c,\downarrow}^{\dagger}\hat{c}_{c',\downarrow}\hat{c}_{c',\uparrow} + \text{h.c.}\right) + \frac{1}{2}\sum_{c(\neq)c';\sigma} J(c,c')\hat{c}_{c,\sigma}^{\dagger}\hat{c}_{c',\bar{\sigma}}^{\dagger}\hat{c}_{c,\bar{\sigma}}\hat{c}_{c',\sigma} \\
&\quad + \Bigg[\sum_{t;\sigma,\sigma'}(T(t) - \delta_{\sigma,\sigma'}A(t))\hat{n}_{t,\sigma}\hat{c}_{u,\sigma'}^{\dagger}\hat{c}_{v,\sigma'} \\
&\qquad + \sum_{t,\sigma}A(t)\left(\hat{c}_{t,\sigma}^{\dagger}\hat{c}_{t,\bar{\sigma}}^{\dagger}\hat{c}_{u,\bar{\sigma}}\hat{c}_{v,\sigma} + \hat{c}_{t,\sigma}^{\dagger}\hat{c}_{u,\bar{\sigma}}^{\dagger}\hat{c}_{t,\bar{\sigma}}\hat{c}_{v,\sigma}\right) \\
&\qquad + \sum_{t(\neq)t'(\neq)t''}\sum_{e,\sigma,\sigma'}S(t,t';t'',e)\hat{c}_{t,\sigma}^{\dagger}\hat{c}_{t',\sigma'}^{\dagger}\hat{c}_{t'',\sigma'}\hat{c}_{e,\sigma} + \text{h.c.}\Bigg].
\end{aligned}
\tag{83}
$$

Here, $t = \zeta, \eta, \xi$ and $e = u, v$ are indices for the three t_{2g} orbitals with symmetries $\zeta = xy$, $\eta = xz$, and $\xi = yz$, and the two e_g orbitals with symmetries $u = 3z^2 - r^2$ and $v = x^2 - y^2$, respectively. The parameters $A(t)$, $T(t)$, $S(t,t';t'',e)$ in eq. (83) are of the same order of magnitude as the exchange interactions $J(c,c')$ and, hence, there is no a-priori reason to neglect $V_{\text{loc}}^{\text{n.dens.}}$. Of all the parameters $U(c,c')$, $J(c,c')$, $A(t)$, $T(t)$, $S(t,t';t'',e)$ only ten are independent in cubic symmetry, see appendix A.2 and Ref. [17].

When we assume that all $3d$-orbitals have the same radial wave-function ('spherical approximation'), all parameters are determined by, e.g., the three Racah parameters A, B, C, see appendix A.2. For comparison with other work, we introduce the average Coulomb interaction between electrons in the same $3d$-orbitals, $U = \sum_c U(c,c)/5 = A + 4B + 3C$, the average Coulomb interaction between electrons in different orbitals, $U' = \sum_{c<c'} U(c,c')/10 = A - B + C$, and the average Hund's-rule exchange interaction, $J = \sum_{c<c'} J(c,c')/10 = 5B/2 + C$ that are related by the symmetry relation $U' = U - 2J$, see appendix A.2. Due to this symmetry relation, the three values of U, U', and J do not determine the Racah parameters A, B, C uniquely. Therefore, we make use of the relation $C/B = 4$ which is a reasonable assumption for metallic nickel [8, 26]. In this way, the three Racah parameters and, consequently, all parameters in $\hat{V}_{\text{loc}}^{\text{full}}$ are functions of U and J, $A = U - 32J/13$, $B = 2J/13$, $C = 8J/13$. This permits a meaningful comparison of our results for all local Hamiltonians.

3.4.2 Double counting corrections

There exists no systematic (let alone rigorous) derivation of the double-counting corrections in eq. (43). A widely used form for this operator has first been introduced in the context of the

LDA+U method. Its expectation value is given by

$$V_{\text{dc}}^{\text{G}} = \frac{\overline{U}}{2}\bar{n}(\bar{n}-1) - \frac{\overline{J}}{2}\sum_{\sigma}\bar{n}_{\sigma}(1-\bar{n}_{\sigma}) \, , \qquad (84)$$

where $\bar{n}_{\sigma} \equiv \sum_{c=1}^{N_c} C_{c,c;\sigma}^{\text{G}}$, $\bar{n} \equiv \bar{n}_{\uparrow} + \bar{n}_{\downarrow}$, and N_c is the number of correlated orbitals ($N_c = 5$ for nickel). Moreover, $\overline{U} = (U + 4U')/5$ and $\overline{J} = \overline{U} - U' + J$. Here,

$$C_{c,c;\sigma}^{\text{G}} = \frac{\langle \Psi_{\text{G}}|\hat{c}_{\mathbf{R},c,\sigma}^{+}\hat{c}_{\mathbf{R},c,\sigma}|\Psi_{\text{G}}\rangle}{\langle \Psi_{\text{G}}|\Psi_{\text{G}}\rangle} = \langle \Phi|\hat{c}_{\mathbf{R},c,\sigma}^{+}\hat{c}_{\mathbf{R},c,\sigma}|\Phi\rangle \qquad (85)$$

is the σ-electron density for the correlated $3d$ orbital c in the Gutzwiller wavefunction. Note that the second equality only holds in the limit of infinite dimensions for our e_g-t_{2g} orbital structure [12].

3.4.3   Size of optimal atomic parameters

Before we proceed, we briefly comment on our optimal Coulomb parameters for nickel and iron because they are substantially larger than the parameters used in other studies [27–31]. For example, for iron the values $U = 2\,\text{eV} \ldots 3\,\text{eV}$ and $J = 0.8\,\text{eV} \ldots 1.0\,\text{eV}$ are used, e.g., to describe the high-temperature regime with the transition from fcc iron to bcc iron and the Curie transition from non-magnetic to magnetic bcc iron, while more recent LDA+DMFT studies employ larger values, $\bar{U} = 4.3\,\text{eV}$, $\widetilde{J} = 1.0\,\text{eV}$ [32].

First of all, we note that the large spread of values of (U, J) in the literature is due to the strong sensitivity of these parameters to the energy window used for projecting, or *downfolding*, the full electronic structure to an effective many-body model [33]. It is well known that the bare Hubbard parameters U are of the order of 20 eV, or larger [3]. They apply for instantaneous charge excitations of an isolated atom, which are strongly screened in a solid. In Fe, for example, the screening reduces U to ~ 3 eV for d-only models [34, 35]. Our self-consistent DFT method is based on a projective technique to construct Wannier functions. In the present calculations, we chose a large energy window, which ensures a very good localization of the $3d$ orbitals, and a minimal dependence of the basis set on atomic positions. This large energy window translates into larger values of U, J [36]. Other calculations can typically afford to retain fewer bands.

Second, we note that the Hubbard-U in our Gutzwiller treatment parameterizes the interaction of two electrons in the same orbital, see appendix A.2. In other approaches, this quantity describes some orbital average. For example, Pourovskii et al. [32] use the Slater-Condon parameter $F^{(0)} = \bar{U}$, where $\bar{U} = (U + 4U')/5$, and $U' = A - B + C = U - 2J$ is the inter-orbital Coulomb repulsion. Naturally, the intra-orbital U is larger than an average over intra-orbital and inter-orbital Coulomb repulsions. Likewise, we work with the average Hund's-rule coupling $J = 5B/2 + C$, see appendix A.2, whereas $\widetilde{J} \equiv (F^{(2)} + F^{(4)})/14 = 7B/2 + 7C/5 = 7J/5$ [32]. Therefore, $F^{(0)} = 4.3\,\text{eV}$ and $\widetilde{J} = 1.0\,\text{eV}$ correspond to $J = 0.71\,\text{eV}$ and $U = \bar{U} + 8\widetilde{J}/7 = 5.4\,\text{eV}$ with $J/U = 0.13$. We note in passing that we work with $C/B = 4$ whereas others use $F^{(2)}/F^{(4)} = 8/5$ which corresponds to $C/B = 175/47 \approx 3.7$ [37].

Lastly, in our Gutzwiller calculations, we use parameters such as U and J to 'match' selected experimental quantities. In this way, we compensate approximations in the model setup, e.g., the neglect of non-local correlations in Hubbard-type models, and in the model analysis, e.g., the limit of infinite dimensions or an approximate variational ground state. For example, in Gutzwiller calculations, the optimal Coulomb parameters must be chosen somewhat smaller when the full atomic interaction is replaced by density-density interactions only [35]. Similarly, larger U-values are found to be optimal when the impurity solver in Quantum-Monte-Carlo is rotationally invariant [27]. Our substantial Hubbard interaction leads to noticeable bandwidth renormalizations and an increase of the quasi-particle masses at the Fermi energy, as seen in experiment [38, 39].

4   Results for transition metals

In this section we compile recent results for nickel and iron as obtained from the Gutzwiller DFT [12, 13].

4.1   Nickel

As a variational approach, the Gutzwiller DFT is expected to be most suitable for the calculation of ground-state properties such as the lattice constant, the magnetic moment, or the Fermi surface of a Fermi liquid. Although more speculative than the ground-state calculations, it is also common to interpret the eigenvalues of the Gutzwiller–Kohn-Sham Hamiltonian $\varepsilon_{\mathrm{n},\sigma}^{\mathrm{G}}(\mathbf{k})$ as the dispersion of the single-particle excitations [40].

4.1.1   Lattice constant, magnetic moment, and bulk modulus of nickel

In Fig. 1, we show the lattice constant and the magnetic moment as a function of U ($1\,\mathrm{eV} \leq U \leq 14\,\mathrm{eV}$) for four different values of J/U ($J/U = 0$, 0.05, 0.075, 0.10). As is well known, the DFT-LDA underestimates the lattice constant, $a_0^{\mathrm{LDA}} = 6.47\,a_{\mathrm{B}}$ is considerably smaller than the experimental value of $a_0 = 6.66\,a_{\mathrm{B}}$ where $a_{\mathrm{B}} = 0.529177\,\text{Å}$ is the Bohr radius. Fig. 1 shows that the Hubbard interaction U increases the lattice constant whereby the Hund's-rule exchange J diminishes the slope. Apparently, a good agreement with the experimental lattice constant requires substantial Hubbard interactions, $U > 10\,\mathrm{eV}$. The increase of the lattice parameter as a function of the Hubbard interaction is readily understood because the $3d$ bandwidth is reduced by electronic correlations so that the $3d$ electrons contribute less to the metallic binding.

Fig. 1 shows the well-known fact that DFT-LDA reproduces the experimental value for the spin-only magnetic moment m_{so} very well, $m_{\mathrm{so}}^{\mathrm{LDA}} = 0.58\mu_{\mathrm{B}}$ vs. $m_{\mathrm{so}}^{\mathrm{exp}} = 0.55\mu_{\mathrm{B}}$. However, when the DFT-LDA calculation is performed for the experimental value of the lattice constant, the magnetic moment is grossly overestimated. As seen in Fig. 1, the Gutzwiller DFT allows us to reconcile the experimental findings both for the lattice constant and the magnetic moment if we work in the parameter range $11\,\mathrm{eV} < U < 14\,\mathrm{eV}$ and $0.05 < J/U < 0.07$. Note that a
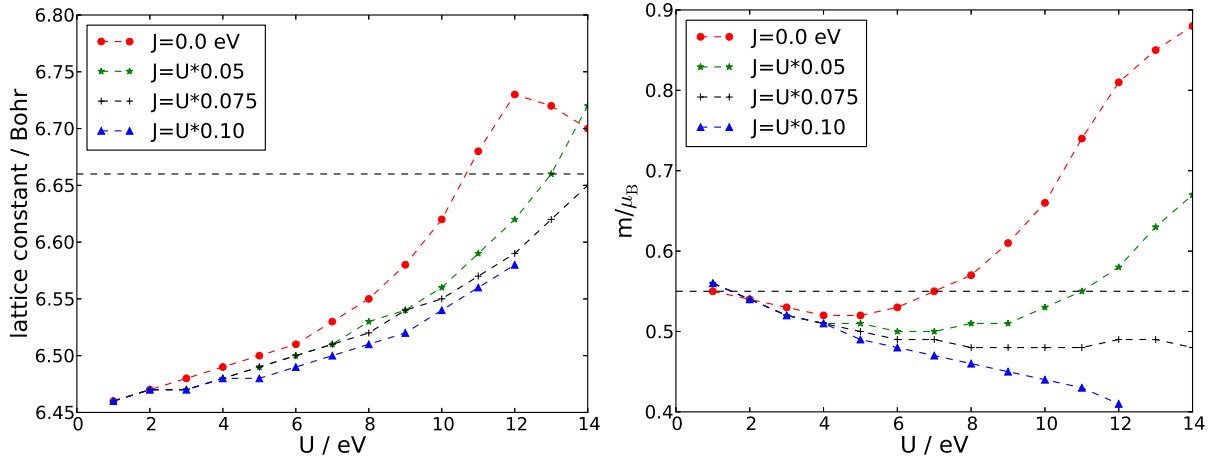
Fig. 1: *Lattice constant (left) and magnetic moment (right) of nickel as a function of U, for four different values of J/U; dashed horizontal lines: experimental values.*

'fine-tuning' of parameters is not required to obtain a reasonable agreement between theory and experiment for the lattice constant and spin-only magnetic moment.

For nickel, detailed information about the quasi-particle bands is available. The quasi-particle dispersion at various high-symmetry points in the Brillouin zone is more sensitive to the precise values of U and J. As we shall show below in more detail, we obtain a satisfactory agreement with ARPES data for the choice ($U^{\mathrm{opt}} = 13\,\mathrm{eV}$, $J^{\mathrm{opt}} = 0.9\,\mathrm{eV}$) with an uncertainty of ± 1 in the last digit. For our optimal values we show in Fig. 2 the ground-state energy per particle $E(a)/N$ as a function of the fcc lattice constant a together with a second-order polynomial fit. The minimum is obtained at $a_0 = 6.63 a_{\mathrm{B}}$, in good agreement with the experimental value $a_0^{\mathrm{exp}} = 6.66 a_{\mathrm{B}}$. For the magnetic spin-only moment we obtain $m_{\mathrm{so}} = 0.52 \mu_{\mathrm{B}}$, in good agreement with the experimental value $m_{\mathrm{so}}^{\mathrm{exp}} = 0.55 \mu_{\mathrm{B}}$.

From the curvature of $E(a)/N$ at $a = a_0$ we can extract the bulk modulus. The bulk modulus at zero temperature is defined as the second-derivative of the ground-state energy with respect to the volume,

$$K = V_0 \left. \frac{\mathrm{d}^2 E(V)}{\mathrm{d}V^2} \right|_{V=V_0} . \tag{86}$$

This implies the Taylor expansion $E(V) = E(V_0) + (K V_0/2)(V/V_0 - 1)^2 + \ldots$ for the ground-state energy as a function of the volume $V = a^3$ (Birch-Murnaghan fit). For the ground-state energy per particle we can thus write $E(a)/N = E(a_0)/N + e_2(a/a_{\mathrm{B}} - a_0/a_{\mathrm{B}})^2 + \ldots$ with

$$e_2 = \frac{9}{8} K a_{\mathrm{B}}^3 (a_0/a_{\mathrm{B}}) , \tag{87}$$

where we took into account that the fcc unit cell hosts four atoms, $V_0 = N a_0^3/4$. The fit leads to $K = 169\,\mathrm{GPa}$, in good agreement with the experimental value, $K = 182\,\mathrm{GPa}$ [41]. It is a well-known fact that the DFT-LDA overestimates the bulk modulus of nickel. Indeed, DFT-LDA gives $K^{\mathrm{LDA}} = 245\,\mathrm{GPa}$.
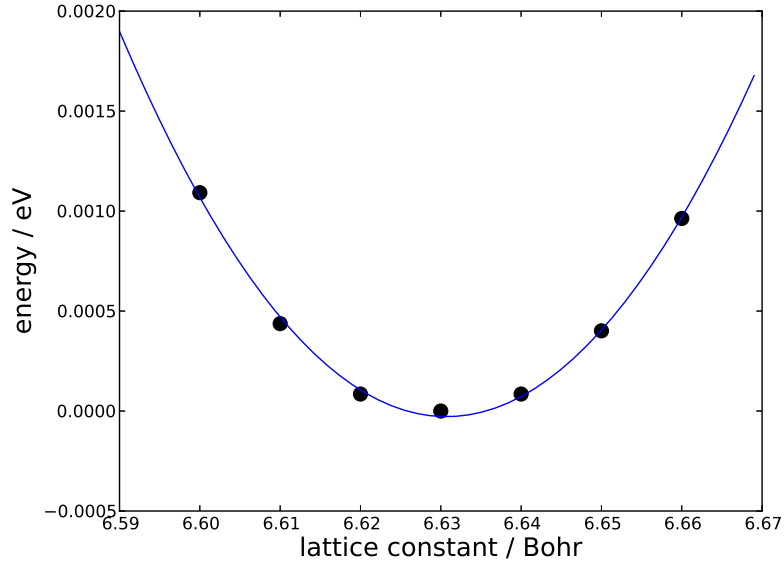
Fig. 2: *Ground-state energy per particle $E_0(a)/N$ relative to its value at $a = 6.63 a_{\rm B}$ as a function of the fcc lattice parameter $a/a_{\rm B}$ in units of the Bohr radius $a_{\rm B}$ for ($U^{\rm opt} = 13\,{\rm eV}$, $J^{\rm opt} = 0.9\,{\rm eV}$). Full line: second-order polynomial fit.*

4.1.2   Quasi-particle bands of nickel

In Fig. 3 we show the quasi-particle band structure of fcc nickel for ($U^{\rm opt} = 13\,{\rm eV}$, $J^{\rm opt} = 0.9\,{\rm eV}$). The most prominent effect of the Gutzwiller correlator is the reduction of the $3d$ bandwidth. From a paramagnetic DFT-LDA calculation one can deduce $W^{\rm LDA} = 4.5\,{\rm eV}$ [42–44], whereas we find $W = 3.3\,{\rm eV}$, in agreement with experiment.
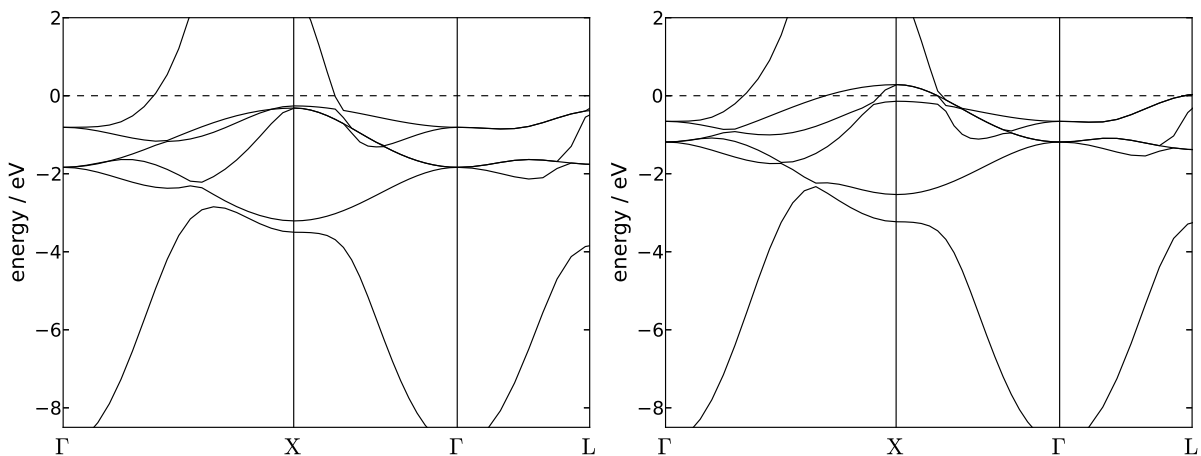

Fig. 3: *Quasi-particle band structure of fcc nickel along high-symmetry lines in the first Brillouin zone for ($U^{\rm opt} = 13\,{\rm eV}$, $J^{\rm opt} = 0.9\,{\rm eV}$). Left: majority spin; Right: minority spin. The Fermi energy is at $E_{\rm F}^{\rm G} = 0$.*

Symmetry	Experiment	Gutzwiller-DFT
$\langle \Gamma_1 \rangle$	8.90 ± 0.30	$8.95[0.08]$
$\langle \Gamma_{25'} \rangle$	1.30 ± 0.06	$1.51[0.65]$
$\langle \Gamma_{12} \rangle$	0.48 ± 0.08	$0.73[0.15]$
$\langle X_1 \rangle$	3.30 ± 0.20	$3.37[0.27]$
$\langle X_3 \rangle$	2.63 ± 0.10	$2.87[0.68]$
$X_{2\uparrow}$	0.21 ± 0.03	0.26
$X_{2\downarrow}$	0.04 ± 0.03	0.14
$X_{5\uparrow}$	0.15 ± 0.03	0.32
$\Delta_{e_g}(X_2)$	0.17 ± 0.05	0.12
$\Delta_{t_{2g}}(X_5)$	0.33 ± 0.04	0.60
$\langle L_1 \rangle$	3.66 ± 0.10	$3.49[0.61]$
$\langle L_3 \rangle$	1.43 ± 0.07	$1.58[0.38]$
$L_{3\uparrow}$	0.18 ± 0.03	0.37
$\langle L_{2'} \rangle$	1.00 ± 0.20	$0.14[0.06]$
$\langle \Lambda_{3;1/2} \rangle$	$0.50[0.21 \pm 0.02]$	$0.64[0.30]$

Table 1: *Quasi-particle band energies for fcc nickel with respect to the Fermi energy in eV at various high-symmetry points (counted positive for occupied states). $\langle \ldots \rangle$ indicates the spin average, error bars in the experiments without spin resolution are given as $\pm$. Theoretical data show the spin average and the exchange splittings in square brackets. $\Lambda_{3;1/2}$ denotes the point half-way on the Λ-line that links the points Γ and L. The first column gives experimental data compiled in [8], the second column gives the result from Gutzwiller DFT at ($U^{\mathrm{opt}} = 13\,\mathrm{eV}, J^{\mathrm{opt}} = 0.9\,\mathrm{eV}$).*

A more detailed comparison of the quasi-particle band structure with experiment is given in table 1. The overall agreement between experiment and theory is quite satisfactory. In particular, only one hole ellipsoid is found at the X-point, in agreement with experiment and in contrast to the DFT-LDA result [8].

We comment on two noticeable discrepancies between theory and experiment. First, the energy of the band $L_{2'}$ at the L-point deviates by a factor of five. This is an artifact that occurs already at the DFT-LDA level and is not cured by the Gutzwiller approach. Since the level has pure $3p$ character around the L point, the origin of the discrepancy is related to the uncertainties in the partial charge densities n_{3d}, $n_{3p,3s}$ in the $3d$ and $3p/3s$ bands. Second, the Gutzwiller DFT prediction for the exchange splitting $\Delta_{t_{2g}}(X_5)$ of the t_{2g} bands at the X-point is a factor of two larger than in experiment. This deviation is related to the fact that, quite generally, all bands are slightly too low in energy. This can be cured by decreasing U and increasing J but this deteriorates the values for the lattice constant and the magnetic moment. We suspect that the deviations are partly due to the use of a heuristic double-counting correction and the neglect of the spin-orbit coupling. Moreover, we expect the results for the band structure to improve when we replace the "poor-man's Wannier" orbitals for the correlated $3d$ electrons by more sophisticated localized wave functions.

4.2 Iron

The ground state of iron poses a difficult problem because the local-density approximation to density functional theory predicts a face-centered cubic (fcc) or a hexagonal closed-packed (hcp) ground state [45, 46]. Gutzwiller-DFT finds the correct (magnetic) body-centered cubic crystal structure without resorting to generalized gradient corrections (GGA) [47, 48].

4.2.1 Lattice constant, magnetic moment, and bulk modulus of iron

When we use $(U = 9\,\mathrm{eV}, J = 0.54\,\mathrm{eV})$ for iron, we find the lattice parameter $a = 5.39 a_\mathrm{B} = 2.85\,\text{Å}$ and the magnetic moment $m = 2.24\mu_\mathrm{B}$ that agree very well with the experimental values, $a_\mathrm{exp} = 5.42 a_\mathrm{B} = 2.87\,\text{Å}$ [49] and $\mu_\mathrm{exp} = 2.22\mu_\mathrm{B}$ [50]. In Fig. 4 we show the ground-state energy per atom, $e(v) = E(V)/N$, as a function of the unit-cell volume $v = V/N = a^3/2$ in the vicinity of the optimal value $v_0 = a^3/2 = 78.3 a_\mathrm{B}^3 = 11.6\,\text{Å}^3$.

As is seen, the magnetic bcc iron phase is energetically favorable over the non-magnetic hcp phase, as found experimentally. Within the Gutzwiller DFT this effect is seen to be the consequence of electronic correlations, not of generalized gradient corrections (GGA) to the LDA functional. Moreover, Fig. 4 suggests that a transition from magnetic bcc iron to non-magnetic hcp iron is possible upon reducing the lattice volume. Such a pressure-induced first-order phase transition is indeed observed experimentally at $p_c^\mathrm{exp} = 10\ldots15\,\mathrm{GPa}$ [51] at room temperature. In Gutzwiller-DFT the critical pressure is higher, $p_c \approx 40\,\mathrm{GPa}$, where entropy effects from magnons and phonons are not included.
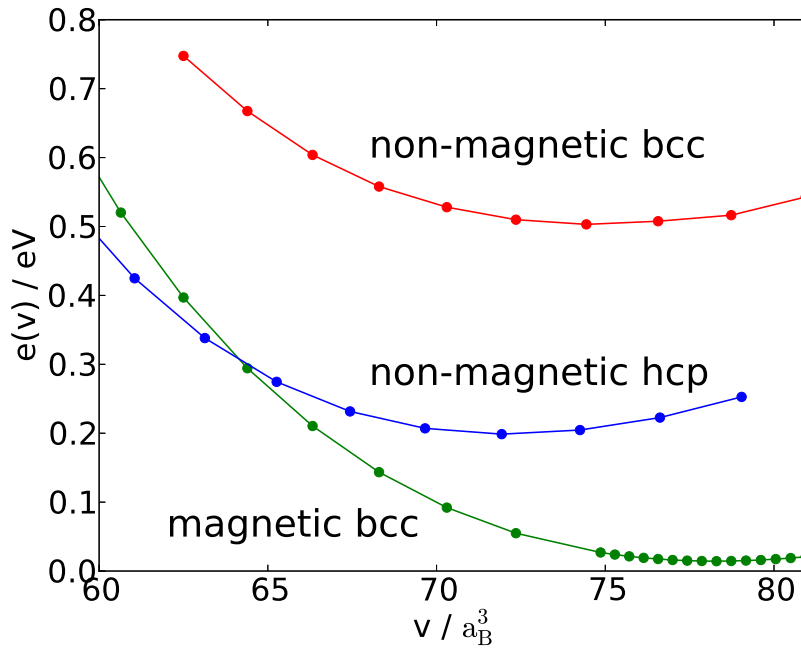

Fig. 4: *Energy per atom $e(v)$ in units of eV as a function of the unit-cell volume v in units of a_B^3 for non-magnetic and ferromagnetic bcc iron and non-magnetic hcp iron for $U = 9\,\mathrm{eV}$ and $J = 0.54\,\mathrm{eV}$, and ambient pressure. The energies are shifted by the same constant amount.*
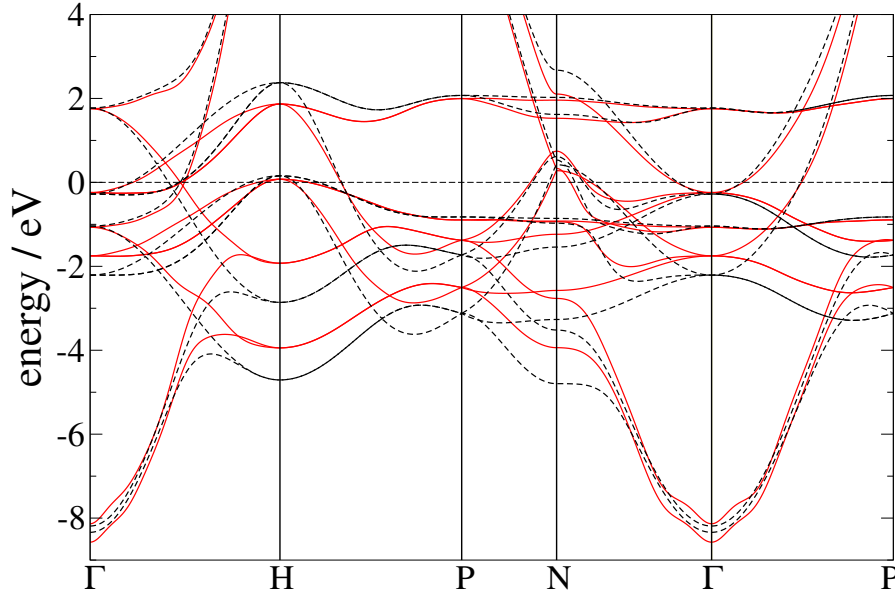
Fig. 5: *Comparison between DFT(GGA) bands (black, dashed lines) and bands from Gutzwiller-DFT (red, full lines) for ($U = 9.0$ eV, $J = 0.54$ eV) for ferromagnetic bcc iron. For clarity, we do not discriminate between majority and minority spin bands. The Fermi energy is at $E_{\mathrm{F}} = 0$ (dashed horizontal line).*

In Gutzwiller-DFT we find a bulk modulus of $B = 165$ GPa, in very good agreement with the experimental value, $B^{\mathrm{exp}} = (170 \pm 4)$ GPa [52,49]. The LDA+Gutzwiller value substantially improves the DFT(LDA) value of $B^{\mathrm{LDA}} = 227$ GPa, it is slightly better than the values from DFT(GGA) studies, $B^{\mathrm{GGA}} = (190 \pm 10)$ GPa [49], and agrees with the value obtained in DMFT calculations, $B^{\mathrm{DMFT}} = 168$ GPa [32].

4.2.2 Quasi-particle bands of ferromagnetic bcc iron

We show the bandstructure for ferromagnetic bcc iron from Gutzwiller-DFT for ($U = 9.0$ eV, $J = 0.54$ eV) in comparison with those from (scalar relativistic) DFT(GGA) calculations in Fig. 5. The DFT(GGA) provides the same equilibrium lattice parameter as used in Gutzwiller-DFT, $a = 5.39 a_{\mathrm{B}}$. The correlations in the Gutzwiller approach lead to an additional bandwidth reduction of the d bands across the Brillouin zone. The uncorrelated, $4sp$-type parts of the quasi-particle bands deep below the Fermi energy do not differ much, e.g., the lowest $4sp$-type majority bands at the Γ point, about 9 eV below the Fermi energy.

The bandwidth reduction in iron is not as strong as in nickel. Nevertheless, for selected symmetry points, the discrepancies between the quasi-particle bands from DFT and Gutzwiller-DFT are quite large, see Fig. 5. For example, at the H-point in the Brillouin zone we find a bandwidth reduction for the majority band by 36%, from $H_{\mathrm{low},\uparrow}^{\mathrm{LDA}} = 5.38$ eV down to $H_{\mathrm{low},\uparrow}^{\mathrm{G\text{-}DFT}} = 3.94$ eV, in good agreement with experiment, $H_{\mathrm{low},\uparrow} = 3.8$ eV [53]. Likewise, at the N-point in the Brillouin zone there is a majority spin band at $N_{\mathrm{low},\uparrow} = 4.5$ eV below the Fermi energy in experiment [53], in comparison with $N_{\mathrm{low},\uparrow}^{\mathrm{LDA}} = 5.47$ eV in DFT(LDA) and $N_{\mathrm{low},\uparrow}^{\mathrm{G\text{-}DFT}} = 3.90$ eV in Gutzwiller-DFT. A comparison of the Landau-Gutzwiller quasi-particle bands and experimental ARPES data close to the Fermi energy can be found in Ref. [13].

5   Summary and outlook

In this work, we presented a detailed derivation of the Gutzwiller Density Functional Theory. Unlike previous studies, our formalism covers all conceivable cases of symmetries and Gutzwiller wave functions. Moreover, our theory is not based on the 'Gutzwiller approximation' which corresponds to an evaluation of expectation values in the limit of infinite lattice coordination number. It is only in the last step that we resort to this limit.

In particular, our derivation consists of three main steps.

1. The density functional of the full many-particle system is related to that of a reference system with local Coulomb interactions in the correlated orbitals. This generalizes the widely used Kohn-Sham scheme, where a single-particle reference system is used, to the Kohn-Sham–Hubbard approach that may be analyzed by sophisticated many-particle methods.

2. In this work, the energy functional of the Hubbard-type reference system is (approximately) evaluated by means of Gutzwiller variational wave functions.

3. Analytical results for the Gutzwiller energy functional are derived in the limit of large coordination number.

We studied the electronic properties of ferromagnetic nickel and iron. The Gutzwiller DFT resolves the main deficiencies of DFT(LDA) in describing ground-state properties such as the lattice constant, the magnetic moment, or the bulk modulus of nickel and iron. In particular, Gutzwiller-DFT gives the proper bcc ground-state structure for iron, without resorting to generalized gradient corrections. Note that our approach requires relatively large values for the local Coulomb interaction, $U = \mathcal{O}(10\,\mathrm{eV})$, to obtain good agreement with experiments.

Our results for the quasi-particle band structure are satisfactory. A perfect agreement with ARPES data would be surprising because we calculate these quantities based on Fermi-liquid assumptions that are strictly valid only in the vicinity of the Fermi surface. The quasi-particle energies strongly depend on the orbital occupations that are influenced by the double-counting corrections. We consider the arbitrariness of the double-counting corrections as the main shortcoming of the Gutzwiller DFT in its present form that should be addressed in future studies.

The method presented in this work can be developed further in various directions. On the level of the Gutzwiller approximation, a number of implementations is still on the agenda, e.g., the inclusion of spin-orbit coupling or the study of phonons. To tackle unconventional superconductivity as seen, e.g., in the cuprates, one has to go beyond the Gutzwiller approximation, see Refs. [18–20] for the single-band model and Ref. [21] for multi-band models. These approaches can be combined with the DFT as explained in Sect. 3. Finally, a time-dependent Gutzwiller method can be used for the calculation of two-particle Green functions, see Refs. [54–56], and references therein. As a long-term perspective, a combination of these methods and the Hubbard-Kohn-Sham Hamiltonian would permit a first-principles calculation of important experimental quantities such as the magnetic susceptibility.

A Appendix

A.1 Single-particle systems

A.1.1 Single-particle density matrix

With the help of a single-particle basis $|k\rangle$ in which a given single-particle operator $\hat{H}_{\text{sp}}$ is diagonal, an eigenstate can be written as

$$|\Phi\rangle = \prod_k {}' \hat{b}_k^\dagger |\text{vac}\rangle \; , \tag{88}$$

where the prime indicates that N single-particle states are occupied in $|\Phi\rangle$. The single-particle density matrix is diagonal in $|\Phi\rangle$,

$$\rho_{k,k'} \equiv \langle \Phi | \hat{b}_k^\dagger \hat{b}_{k'} | \Phi \rangle = \delta_{k,k'} f_k \; , \tag{89}$$

and the entries on the diagonal obey $f_k^2 = f_k$ because we have $f_k = 0, 1$. Therefore, we have shown that

$$\tilde{\rho} \cdot \tilde{\rho} = \tilde{\rho} \; . \tag{90}$$

Since the operators $\hat{c}_i^\dagger$ for any other single-particle basis and the operators $\hat{b}_k^\dagger$ are related via a unitary transformation, eq. (33) holds generally for single-particle density matrices for single-particle product states.

A.1.2 Minimization with respect to the single-particle density matrix

We consider a general real function $E(\tilde{\rho})$ of a non-interacting density matrix $\tilde{\rho}$ with the elements

$$\rho_{i,j} = \langle \Phi | \hat{c}_j^\dagger \hat{c}_i | \Phi \rangle \; . \tag{91}$$

The fact that $\tilde{\rho}$ is derived from a single-particle product wave function $|\Phi\rangle$ is equivalent to the matrix equation (90). Hence, the minimum of $E(\tilde{\rho})$ in the 'space' of all non-interacting density matrices is determined by the condition

$$\frac{\partial}{\partial \rho_{j,i}} L(\tilde{\rho}) = 0 \; , \tag{92}$$

where we introduced the 'Lagrange functional'

$$L(\tilde{\rho}) \equiv E(\tilde{\rho}) - \sum_{l,m} \Omega_{l,m} \left(\sum_p \rho_{m,p} \rho_{p,l} - \rho_{m,l} \right) \tag{93}$$

and the matrix $\widetilde{\Omega}$ of Lagrange parameters $\Omega_{l,m}$. Eq. (92) leads to the matrix equation

$$\tilde{H} = \tilde{\rho} \cdot \widetilde{\Omega} + \widetilde{\Omega} \cdot \tilde{\rho} - \widetilde{\Omega} \tag{94}$$

for the 'Hamilton matrix' $\tilde{H}$ with the elements

$$H_{i,j} = \frac{\partial}{\partial \rho_{j,i}} E(\tilde{\rho}) \; . \tag{95}$$

Equation (94) is satisfied if eq. (90) holds and if

$$[\tilde{H}, \tilde{\rho}] = 0 \; . \tag{96}$$

Hence, $\tilde{H}$ and $\tilde{\rho}$ must have the same basis of (single-particle) eigenvectors and, consequently, we find an extremum of $E(\tilde{\rho})$ if we choose $|\Phi\rangle$ as an eigenstate of

$$\hat{H}_{\mathrm{sp}} = \sum_{i,j} H_{i,j} \hat{c}_i^\dagger \hat{c}_j \; . \tag{97}$$

Usually, $|\Phi\rangle$ can be chosen as the ground state of $\hat{H}_{\mathrm{sp}}$.

A.1.3   Basis sets

In the following we assume that the potential is lattice periodic,

$$V_\sigma^{\mathrm{KS}}(\mathbf{r}) = U(\mathbf{r}) + V_{\mathrm{Har}}(\mathbf{r}) + v_{\mathrm{sp,xc},\sigma}(\mathbf{r}) = V_\sigma^{\mathrm{KS}}(\mathbf{r} + \mathbf{R}) \; , \tag{98}$$

where $\mathbf{R}$ is a lattice vector. The Fourier components are finite for reciprocal lattice vectors $\mathbf{G}$ only,

$$V_{\mathbf{G},\sigma}^{\mathrm{KS}} = \frac{1}{V} \int \mathrm{d}\mathbf{r}\, V_\sigma^{\mathrm{KS}}(\mathbf{r}) e^{-\mathrm{i}\mathbf{G}\cdot\mathbf{r}} \; , \tag{99}$$

where V is the crystal volume. As a consequence of the lattice periodicity, the crystal momentum $\mathbf{k}$ from the first Brillouin zone is a good quantum number.

As seen from eq. (41), the Kohn-Sham Hamiltonian is diagonalized for the single-particle states $\psi_{\mathbf{k},\mathrm{n},\sigma}(\mathbf{r}) = \langle\mathbf{r}|\mathbf{k}, \mathrm{n}, \sigma\rangle$ that obey the Kohn-Sham equations [1] (n: band index)

$$h_\sigma^{\mathrm{KS}}(\mathbf{r})\psi_{\mathbf{k},\mathrm{n},\sigma}(\mathbf{r}) = \varepsilon_{\mathrm{n},\sigma}(\mathbf{k})\psi_{\mathbf{k},\mathrm{n},\sigma}(\mathbf{r}) \; . \tag{100}$$

In its eigenbasis, the Kohn-Sham Hamiltonian takes the form

$$\hat{H}^{\mathrm{KS}} = \sum_{\mathbf{k},\mathrm{n},\sigma} \varepsilon_{\mathrm{n},\sigma}(\mathbf{k}) \hat{b}_{\mathbf{k},\mathrm{n},\sigma}^\dagger \hat{b}_{\mathbf{k},\mathrm{n},\sigma} \; . \tag{101}$$

Its ground state is given by

$$|\Phi_0\rangle = \prod_\sigma \prod_{\mathbf{k},\mathrm{n}} {}' \hat{b}_{\mathbf{k},\mathrm{n},\sigma}^\dagger |\mathrm{vac}\rangle \; , \tag{102}$$

where the N levels lowest in energy are occupied as indicated by the prime at the product, $\varepsilon_{\mathrm{n},\sigma}(\mathbf{k}) \leq E_{\mathrm{F},\sigma}$. Then,

$$f_{\mathbf{k},\mathrm{n},\sigma} = \langle\Phi_0|\hat{b}_{\mathbf{k},\mathrm{n},\sigma}^\dagger \hat{b}_{\mathbf{k},\mathrm{n},\sigma}|\Phi_0\rangle = \Theta\left(E_{\mathrm{F},\sigma} - \varepsilon_{\mathrm{n},\sigma}(\mathbf{k})\right) \tag{103}$$

is unity for occupied levels up to the Fermi energy $E_{\mathrm{F},\sigma}$, and zero otherwise.

From eq. (26), the field operators read

$$\hat{\Psi}_\sigma(\mathbf{r}) = \sum_{\mathbf{k},\mathrm{n}} \psi_{\mathbf{k},\mathrm{n},\sigma}(\mathbf{r})\hat{b}_{\mathbf{k},\mathrm{n},\sigma} \quad , \quad \hat{\Psi}_\sigma^\dagger(\mathbf{r}) = \sum_{\mathbf{k},\mathrm{n}} \psi_{\mathbf{k},\mathrm{n},\sigma}^*(\mathbf{r})\hat{b}_{\mathbf{k},\mathrm{n},\sigma}^\dagger \; . \tag{104}$$

Therefore, the ground-state density is readily obtained as

$$n_\sigma^0(\mathbf{r}) = \langle \Phi_0 | \hat{\Psi}_\sigma^\dagger(\mathbf{r}) \hat{\Psi}_\sigma(\mathbf{r}) | \Phi_0 \rangle = \sum_{\mathbf{k},n} f_{\mathbf{k},n,\sigma} |\psi_{\mathbf{k},n,\sigma}(\mathbf{r})|^2 = \langle \mathbf{r} | \sum_{\mathbf{k}} \hat{\rho}_\sigma^{(0)}(\mathbf{k}) | \mathbf{r} \rangle \ ,$$

$$\hat{\rho}_\sigma^{(0)}(\mathbf{k}) = \sum_n f_{\mathbf{k},n,\sigma} | \mathbf{k}, n, \sigma \rangle \langle \mathbf{k}, n, \sigma | \ , \tag{105}$$

see also eq. (31). Since this quantity enters the Kohn-Sham Hamiltonian, its solution must be achieved self-consistently.

In order to make contact with many-particle approaches based on Hubbard-type models, we need to identify orbitals that enter the local two-particle interaction. Implemented plane-wave codes provide the transformation coefficients $F_{(\mathbf{k},n),(\mathbf{R},b);\sigma}$ from Bloch eigenstates $|\mathbf{k}, n, \sigma \rangle$ to orbital Wannier states $|\mathbf{R}, b, \sigma \rangle$,

$$|\mathbf{R}, b, \sigma \rangle = \sum_{\mathbf{k},n} F_{(\mathbf{k},n),(\mathbf{R},b);\sigma} |\mathbf{k}, n, \sigma \rangle \ , \quad F_{(\mathbf{k},n),(\mathbf{R},b);\sigma} = \langle \mathbf{k}, n, \sigma | \mathbf{R}, b, \sigma \rangle \ . \tag{106}$$

The Wannier orbitals

$$\phi_{\mathbf{R},b,\sigma}(\mathbf{r}) = \langle \mathbf{r} | \mathbf{R}, b, \sigma \rangle \tag{107}$$

are maximal around a lattice site $\mathbf{R}$ and the orbital index b resembles atomic quantum numbers, e.g., $b = 3s, 3p, 3d$. In the orbital Wannier basis the field operators are given by

$$\hat{\Psi}_\sigma^\dagger(\mathbf{r}) = \sum_{\mathbf{R},b} \phi_{\mathbf{R},b,\sigma}^*(\mathbf{r}) \hat{c}_{\mathbf{R},b,\sigma}^\dagger \quad , \quad \hat{\Psi}_\sigma(\mathbf{r}) = \sum_{\mathbf{R},b} \phi_{\mathbf{R},b,\sigma}(\mathbf{r}) \hat{c}_{\mathbf{R},b,\sigma} \ , \tag{108}$$

and the Kohn-Sham Hamiltonian in the orbital Wannier basis becomes

$$\hat{H}^{\mathrm{KS}} = \sum_{\mathbf{R},b,\mathbf{R}',b',\sigma} T_{(\mathbf{R},b),(\mathbf{R}',b');\sigma}^{\mathrm{KS}} \hat{c}_{\mathbf{R},b,\sigma}^\dagger \hat{c}_{\mathbf{R}',b',\sigma} \tag{109}$$

with the overlap matrix elements

$$T_{(\mathbf{R},b),(\mathbf{R}',b');\sigma}^{\mathrm{KS}} = \int d\mathbf{r} \ \phi_{\mathbf{R},b,\sigma}^*(\mathbf{r}) h_\sigma^{\mathrm{KS}}(\mathbf{r}) \phi_{\mathbf{R}',b',\sigma}(\mathbf{r}) \ , \tag{110}$$

see eq. (41). These matrix elements appear in a tight-binding representation of the kinetic energy in Hubbard-type models.

We also define the orbital Bloch basis,

$$\phi_{\mathbf{k},b,\sigma}(\mathbf{r}) = \sqrt{\frac{1}{L}} \sum_{\mathbf{R}} e^{i\mathbf{k}\cdot\mathbf{R}} \phi_{\mathbf{R},b,\sigma}(\mathbf{r}) \ ,$$

$$\phi_{\mathbf{R},b,\sigma}(\mathbf{r}) = \sqrt{\frac{1}{L}} \sum_{\mathbf{k}} e^{-i\mathbf{k}\cdot\mathbf{R}} \phi_{\mathbf{k},b,\sigma}(\mathbf{r}) \ , \tag{111}$$

where $\mathbf{k}$ is from the first Brillouin zone and L is the number of lattice sites. The field operators are given by

$$\hat{\Psi}_\sigma^\dagger(\mathbf{r}) = \sum_{\mathbf{k},b} \phi_{\mathbf{k},b,\sigma}^*(\mathbf{r}) \hat{c}_{\mathbf{k},b,\sigma}^\dagger \quad , \quad \hat{\Psi}_\sigma(\mathbf{r}) = \sum_{\mathbf{k},b} \phi_{\mathbf{k},b,\sigma}(\mathbf{r}) \hat{c}_{\mathbf{k},b,\sigma} \ . \tag{112}$$

In the orbital Wannier basis, the Kohn-Sham single-particle Hamiltonian reads

$$\hat{H}^{\mathrm{KS}} = \sum_{\mathbf{k},b,b',\sigma} T^{\mathrm{KS}}_{b,b';\sigma}(\mathbf{k}) \hat{c}^{\dagger}_{\mathbf{k},b,\sigma} \hat{c}_{\mathbf{k},b',\sigma} ,$$

$$T^{\mathrm{KS}}_{b,b';\sigma}(\mathbf{k}) = \int \mathrm{d}\mathbf{r}\, \phi^{*}_{\mathbf{k},b,\sigma}(\mathbf{r}) h^{\mathrm{KS}}_{\sigma}(\mathbf{r}) \phi_{\mathbf{k},b',\sigma}(\mathbf{r}) . \tag{113}$$

A.2 Atomic Hamiltonian in cubic symmetry

We choose the Hubbard parameters $U(u,v), U(\zeta,\zeta), U(\xi,\eta), U(\zeta,u), U(\zeta,v)$, the four Hund's-rule couplings $J(u,v), J(\xi,\eta), J(\zeta,u), J(\zeta,v)$, and the two-particle transfer matrix element $S(\eta,\xi;\zeta,u)$ as our ten independent Coulomb matrix elements in cubic symmetry. The other matrix elements in eq. (83) can be expressed as [26, 17]

$$\begin{aligned}
U(u,u) &= U(v,v) &&= U(u,v) + 2J(u,v) , \\
U(\xi,u) &= U(\eta,u) &&= (U(\zeta,u) + 3U(\zeta,v))/4 , \\
U(\xi,v) &= U(\eta,v) &&= (3U(\zeta,u) + U(\zeta,v))/4 , \\
J(\xi,u) &= J(\eta,u) &&= (J(\zeta,u) + 3J(\zeta,v))/4 , \\
J(\xi,v) &= J(\eta,v) &&= (3J(\zeta,u) + J(\zeta,v))/4 , \\
T(\eta;u,v) &= -T(\xi;u,v) &&= \sqrt{3}(U(\zeta,u) - U(\zeta,v))/4 , \\
A(\eta;u,v) &= -A(\xi;u,v) &&= \sqrt{3}(J(\zeta,u) - J(\zeta,v))/4 , \\
S(\xi,\eta;\zeta,u) &&&= S(\eta,\xi;\zeta,u) , \\
S(\zeta,\xi;\eta,u) &&&= -2S(\eta,\xi;\zeta,u) , \\
S(\xi,\eta;\zeta,v) &&&= -\sqrt{3}S(\eta,\xi;\zeta,u) , \\
S(\zeta,\xi;\eta,u) &&&= \sqrt{3}S(\eta,\xi;\zeta,u) .
\end{aligned} \tag{114}$$

If we further assume that the radial part of the t_{2g}-orbitals and the e_g-orbitals are identical ('spherical approximation'), we may express all matrix elements in terms of three parameters, e.g., the Racah parameters A, B, and C that are related to the Slater-Condon parameters by $A = F^{(0)} - F^{(4)}/9$, $B = (F^{(2)} - 5F^{(4)}/9)/49$, and $C = 5F^{(4)}/63$; inversely, $F^{(0)} = A + 7C/5$, $F^{(2)} = 49B + 7C$, $F^{(4)} = 63C/5$. In particular,

$$\begin{aligned}
U(u,v) &= A - 4B + C , \\
J(u,v) &= 4B + C , \\
U(\zeta,\zeta) &= A + 4B + 3C , \\
U(\xi,\eta) &= A - 2B + C , \\
J(\xi,\eta) &= 3B + C , \\
U(\zeta,u) &= A - 4B + C , \\
U(\zeta,v) &= A + 4B + C , \\
J(\zeta,v) &= C , \\
J(\zeta,u) &= 4B + C , \\
S(\eta,\xi;\zeta,u) &= -\sqrt{3}B .
\end{aligned} \tag{115}$$

The average Coulomb interaction between electrons in same orbitals is given by

$$U = \frac{1}{5} \sum_{c=\xi,\eta,\zeta,u,v} U(c,c) = A + 4B + 3C \,, \tag{116}$$

the average Coulomb interaction between electrons in different orbitals is given by

$$U' = \frac{1}{10} \sum_{c,c'=\xi,\eta,\zeta,u,v;c<c'} U(c,c') = A - B + C \,, \tag{117}$$

and the average Hund's-rule coupling becomes

$$J = \frac{1}{10} \sum_{c,c'=\xi,\eta,\zeta,u,v;c<c'} J(c,c') = \frac{5}{2}B + C \,. \tag{118}$$

These three quantities are not independent but related by the symmetry relation $U' = U - 2J$. This means that by choosing two of these parameters (e.g., U and J) the three Racah parameters, and therefore all the parameters in Eq. (80) are not uniquely defined. Hence, we use the additional relation $C/B = 4$ which is a reasonable assumption for transition metals [26]. It corresponds to $F^{(2)}/F^{(4)} = 55/36 = 1.53$, in agreement with the estimate $F^{(2)}/F^{(4)} \approx 1.60 = 8/5$ by de Groot et al. [37].

References

[1] For an overview, see R.M. Martin, *Electronic Structure* (Cambridge Univ. Press, 2004);
R.M. Dreizler and E.K.U. Gross, *Density Functional Theory* (Springer, Berlin, 1990)

[2] V.L. Moruzzi, J.F. Janak, and A.R. Williams, *Calculated Electronic Properties of Metals*
(Pergamon Press, New York, 1978)

[3] J. Hubbard, Proc. Roy. Soc. A **276**, 238 (1963)

[4] M.C. Gutzwiller, Phys. Rev. Lett. **10**, 159 (1963)

[5] V.I. Anisimov, F. Aryasetiawan, and A.I. Lichtenstein,
J. Phys.: Condens. Matter **9**, 767 (1997)

[6] G. Kotliar, S. Savrasov, K. Haule, V. Oudovenko, O. Parcollet, and C. Marianetti,
Rev. Mod. Phys. **78**, 865 (2006)

[7] E. Pavarini, E. Koch, D. Vollhardt, and A. Lichtenstein (eds.):
The LDA+DMFT approach to strongly correlated materials,
Modeling and Simulation, Vol. 1 (Forschungszentrum Jülich,2 011)
http://www.cond-mat.de/events/correl11

[8] J. Bünemann, F. Gebhard, and W. Weber in A. Narlikar (ed.):
Frontiers in Magnetic Materials (Springer, Berlin, 2005), p. 117.

[9] K.M. Ho, J. Schmalian, and C.Z. Wang, Phys. Rev. B **77**, 073101 (2008); Y.-X. Yao,
J. Schmalian, C.Z. Wang, H.M. Ho, and G. Kotliar, Phys. Rev. B **84**, 245112 (2011);
N. Lanatà, Y.-X. Yao, C.Z. Wang, K.M. Ho, J. Schmalian, K. Haule, and G. Kotliar,
Phys. Rev. Lett. **111**, 196801 (2013)

[10] G.-T. Wang, X. Dai, and Z. Fang, Phys. Rev. Lett. **101**, 066403 (2008); X. Deng, X. Dai,
and Z. Fang, Eur. Phys. Lett. **83**, 37008 (2008); X. Deng, L. Wang, X. Dai, and Z. Fang,
Phys. Rev. B **79**, 075114 (2009); G.-T. Wang, Y. Qian, G. Xu, X. Dai, and Z. Fang,
Phys. Rev. Lett. **104**, 047002 (2010); M.-F. Tian, X. Deng, Z. Fang, and X. Dai,
Phys. Rev. B **84**, 205124 (2011)

[11] R. Dong, X. Wan, X. Dai, and S.Y. Savrasov, Phys. Rev. B **89**, 165122 (2014)

[12] T. Schickling, J. Bünemann, F. Gebhard, and W. Weber, New J. Phys. **16**, 93034 (2014)

[13] T. Schickling, J. Bünemann, F. Gebhard, and L. Boeri, Phys. Rev. B **93**, 205151 (2016)

[14] M. Levy, Phys. Rev. A **26**, 1200 (1982); E.H. Lieb, Int. J. Quan. Chem. **24**, 243 (1983)

[15] The condition (22) is a bit too strong. We can equally work with the functional
$\widetilde{D}_{\mathrm{sp}}\left[\{n_\sigma(\mathbf{r})\}\right] = D_{\mathrm{sp}}\left[\{n_\sigma(\mathbf{r})\}\right] + \Delta\left[\{n_\sigma(\mathbf{r})\}\right]$ as long as we demand $\Delta\left[\{n_\sigma^0(\mathbf{r})\}\right] = 0$ and
$(\partial\Delta\left[\{n_\sigma(\mathbf{r})\}\right])/(\partial n_\sigma(\mathbf{r}))|_{n_\sigma(\mathbf{r})=n_\sigma^0(\mathbf{r})} = 0$. Then, $\widetilde{D}_{\mathrm{sp}}\left[\{n_\sigma(\mathbf{r})\}\right]$ leads to the same ground-
state energy and ground-state density as $D_{\mathrm{sp}}\left[\{n_\sigma(\mathbf{r})\}\right]$.

[16] J. Bünemann Chap. 5 in E. Pavarini, E. Koch, F. Anders, and M. Jarrell (eds.):
Correlated Electrons: From Models to Materials
Modeling and Simulation, Vol. 2 (Forschungszentrums Jülich, 2012)
http://www.cond-mat.de/events/correl12.

[17] J. Bünemann and F. Gebhard, J. Phys.: Condens. Matt. **29**, 165601 (2017)

[18] F. Gebhard, Phys. Rev. B **41**, 9452 (1990)

[19] J. Bünemann, T. Schickling, and F. Gebhard, Europhys. Lett. **98**, 27006 (2012)

[20] J. Kaczmarczyk, J. Spałek, T. Schickling, and J. Bünemann,
Phys. Rev. B **88**, 115127 (2013)

[21] K. zu Münster and J. Bünemann, Phys. Rev. B **94**, 045135 (2016)

[22] J. Bünemann, T. Linneweber, U. Löw, F.B. Anders, and F. Gebhard,
Phys. Rev. B **94**, 035116 (2016)

[23] J. Bünemann, T. Linneweber, and F. Gebhard, phys. stat. sol. (b) **254**, 1600166 (2017)

[24] J. Bünemann, W. Weber, and F. Gebhard, Phys. Rev. B **57**, 6896 (1998)

[25] J. Bünemann, T. Schickling, F. Gebhard, and W. Weber,
physica status solidi (b) **249**, 1282 (2012)

[26] S. Sugano, Y. Tanabe, and H. Kamimura, *Multiplets of Transition-Metal Ions in Crystals*
Pure and Applied Physics **33** (Academic Press, New York, 1970)

[27] A.S. Belozerov and V.I. Anisimov, J. Phys.: Condens. Matt. **26**, 375601 (2014)

[28] A.A. Katanin, A.I. Poteryaev, A.V. Efremov, A.O. Shorikov, S.L. Skornyakov,
M.A. Korotin, and V.I. Anisimov, Phys. Rev. B **81**, 045117 (2010)

[29] I. Leonov, A.I. Poteryaev, V.I. Anisimov, and D. Vollhardt,
Phys. Rev. Lett. **106**, 106405 (2011)

[30] I. Leonov, A.I. Poteryaev, Y.N. Gornostyrev, A.I. Lichtenstein, M.I. Katsnelson,
V.I. Anisimov, and D. Vollhardt, Scientific Reports **4**, 5585 (2014)

[31] A.I. Lichtenstein, M.I. Katsnelson, and G. Kotliar, Phys. Rev. Lett. **87**, 067205 (2001)

[32] L.V. Pourovskii, J. Mravlje, M. Ferrero, O. Parcollet, and I.A. Abrikosov,
Phys. Rev. B **90**, 155120 (2014)

[33] T. Miyake, F. Aryasetiawan, and M. Imada, Phys. Rev. B **80**, 155134 (2009)

[34] T. Schickling, F. Gebhard, and J. Bünemann, Phys. Rev. Lett. **106**, 146402 (2011)

[35] T. Schickling, F. Gebhard, J. Bünemann, L. Boeri, O.K. Andersen, and W. Weber,
Phys. Rev. Lett. **108**, 036406 (2012)

[36] F. Aryasetiawan, K. Karlsson, O. Jepsen, and U. Schönberger,
Phys. Rev. B **74**, 125106 (2006)

[37] F.M.F. de Groot, J.C. Fuggle, B.T. Thole, and G.A. Sawatzky,
Phys. Rev. B **42**, 5459 (1990)

[38] J. Schäfer, M. Hoinkis, E. Rotenberg, P. Blaha, and R. Claessen,
Phys. Rev. B **72**, 155115 (2005)

[39] J. Sánchez-Barriga, J. Fink, V. Boni, I. Di Marco, J. Braun, J. Minár, A. Varykhalov,
O. Rader, V. Bellini, F. Manghi, H. Ebert, M.I. Katsnelson, A.I. Lichtenstein, O. Eriksson,
W. Eberhardt, and H.A. Dürr, Phys. Rev. Lett. **103**, 267203 (2009)

[40] J. Bünemann, F. Gebhard, and R. Thul, Phys. Rev. B **67**, 075103 (2003)

[41] D.-J. Zhao, K. Albe, and H. Hahn, Scripta Materialia **55**, 473 (2006)

[42] J. Bünemann, F. Gebhard, T. Ohm, R. Umstätter, S. Weiser, W. Weber, R. Claessen,
D. Ehm, A. Harasawa, A. Kakizaki, A. Kimura, G. Nicolay, S. Shin, and V.N. Strocov,
Europhys. Lett. **61**, 667 (2003)

[43] J. Bünemann, F. Gebhard, T. Ohm, S. Weiser, and W. Weber,
Phys. Rev. Lett. **101**, 236404 (2008)

[44] A. Hofmann, X. Cui, J. Schäfer, S. Meyer, P. Höpfner, C. Blumenstein, M. Paul, L. Patthey,
E. Rotenberg, J. Bünemann, F. Gebhard, T. Ohm, W. Weber, and R. Claessen,
Phys. Rev. Lett. **102**, 187204 (2009)

[45] C.S. Wang, B.M. Klein, and H. Krakauer, Phys. Rev. Lett. **54**, 1852 (1985)

[46] S.K. Bose, O.V. Dolgov, J. Kortus, O. Jepsen, and O.K. Andersen,
Phys. Rev. B **67**, 214518 (2003)

[47] G. Steinle-Neumann, L. Stixrude, and R.E. Cohen, Phys. Rev. B**60**, 791 (1999)

[48] G.Y. Guo and H.H. Wang, Chin. J. of Phys. **38**, 949 (2000)

[49] H.L. Zhang, S. Lu, M.P.J. Punkkinen, Q.-M. Hu, B. Johansson, and L. Vitos,
     Phys. Rev. B **82**, 132409 (2010)

[50] H. Danan, A. Herr, and A.J.P. Meyer, J. Appl. Phys. **39**, 669 (1968)

[51] D. Bancroft, E.L. Peterson, and S. Minshall, J. Appl. Phys. **27**, 291 (1956)

[52] A.P. Jephcoat, H.K. Mao, and P.M. Bell, J. Geophys. Res.: Solid Earth **91**, 4677 (1986)

[53] A.M. Turner, A.W. Donoho, and J.L. Erskine, Phys. Rev. B **29**, 2986 (1984)

[54] G. Seibold, F. Becca, and J. Lorenzana, Phys. Rev. B **78**, 045114 (2008)

[55] J. Bünemann, M. Capone, J. Lorenzana, and G. Seibold, New J. Phys. **10**, 053050 (2013)

[56] J. Bünemann, S. Wasner, E. von Oelsen, and G. Seibold, Phil. Mag. **95**, 550 (2015)